

1
2
3
4
5
6
7
8
9
10
11
12
13
14
15
16
17
18
19
20
21
22
23
24
25
26
27
28
29
30
31
32
33
34
35
36
37

A review on the global soil property maps for Earth System Models

Yongjiu Dai^{1*}, Wei Shangguan^{1*}, Nan Wei¹, Qinchuan Xin², Hua Yuan¹, Shupeng Zhang¹, Shaofeng Liu¹, Xingji Lu¹, Dagang Wang², Fapeng Yan³

¹ Southern Marine Science and Engineering Guangdong Laboratory (Zhuhai), Guangdong Province Key Laboratory for Climate Change and Natural Disaster Studies, School of Atmospheric Sciences, Sun Yat-sen University, Guangzhou, China.

²School of Geography and Planning, Sun Yat-sen University, Guangzhou, China.

³College of Global Change and Earth System Science, Beijing Normal University, Beijing, China

Correspondence to: Yongjiu Dai (daiyj6@mail.sysu.edu.cn) and Wei Shangguan (shgwei@mail.sysu.edu.cn)

Abstract. Soil is an important regulator of Earth system processes, but remains one of the least well-described data layers in Earth System Models (ESMs). We reviewed global soil property maps from the perspective of ESMs, including soil physical and, chemical and biological properties, which can also offer insights to soil data developers and users. These soil datasets provide model inputs, initial variables and benchmark datasets. For modelling use, the dataset should be geographically continuous, scalable and have uncertainty estimates. The popular soil datasets used in ESMs are often based on limited soil profiles and coarse resolution soil type maps with various uncertainty sources. Updated and comprehensive soil information needs to be incorporated in ESMs. New generation soil datasets derived through digital soil mapping with abundant, harmonized and quality controlled soil observations and environmental covariates are preferred to those derived through the linkage method (i.e., taxotransfer rule-based method) for ESMs. SoilGrids has the highest accuracy and resolution among the global soil datasets, while other recently developed datasets offer useful compensation. Because there is no universal pedotransfer function, an ensemble of them may be more suitable to provide derived soil properties to ESMs. Aggregation and upscaling of soil data are needed for model use but can be avoided by using a subgrid method in ESMs at the expense of increases in model complexity. Producing soil property maps in a time series remains still challenging. The uncertainties in soil data needs to be estimated and incorporated into ESMs.

38 **1 Introduction**

39 Soil or the pedosphere is a key component of the Earth system, and plays an important
40 role in water, energy and carbon balances and other biogeochemical processes. An
41 accurate description of soil properties is essential in modelling capability of Earth
42 System Models (ESMs) to predict land surface processes at the global and regional
43 scales (Luo et al., 2016). Soil information is required by land surface models (LSMs),
44 which are a component of ESMs. With the aid of computer-based geographic systems,
45 many researchers have produced geographical databases to organize and harmonize
46 large amounts of soil information generated from soil surveys during recent decades
47 (Batjes, 2017; Hengl et al., 2017). However, soil datasets used in ESMs are not yet well
48 updated or well utilized (Sanchez et al., 2009; FAO/IIASA/ISRIC/ISS-CAS/JRC, 2012).
49 The popular soil datasets used in ESMs are outdated and have limited accuracies. Some
50 soil properties, such as gravel (or coarse fragment) and depth to bedrock, are not utilized
51 in most ESMs. The ESMs' schemes and structures must be changed to represent soil
52 processes in a more realistic manner when utilizing new soil information (Brunke et al.,
53 2016; Luo et al., 2016; Oleson et al., 2010). For example, Brunke et al. (2016)
54 incorporated the depth to bedrock data in a land surface model using variable soil layers
55 instead of the previous constant depth. Better soil information with a high resolution
56 and better representation of soil in models has improved and will improve the
57 performance of simulating the Earth system (eg., Livneh et al., 2015; Dy and Fung,
58 2016; Kearney and Maino, 2018).

59 ESMs require detailed information on the physical, chemical and biological properties
60 of the soil. Site observations (called soil profiles) from soil surveys include soil
61 properties such as soil depth, soil texture (sand, silt and clay fractions), organic matter,
62 coarse fragments, bulk density, soil colour, soil nutrients (carbon (C), nitrogen (N),
63 phosphorus (P), potassium (K) and sulphur (S)), amount of roots and so on. The range
64 of soil data collected during a soil survey varies with scale, country or regional
65 specifications, and projected applications of the data (i.e., type of soil surveys, routine
66 versus specifically designed surveys). As a result, the availability of soil properties
67 differs in different soil databases. However, soil hydraulic and thermal parameters as
68 well as biogeochemical parameters are usually not observed in soil surveys, which need
69 to be estimated by pedotransfer functions (PTFs) (Looy et al., 2017). This review
70 focuses on soil data (usually single point observations at a given moment in time) from
71 soil surveys, while variables such as soil temperature and soil moisture are beyond the
72 scope of this paper.

73 Soil properties function in three aspects in ESMs:

74 1) Model inputs to estimate parameters. The soil thermal (soil heat capacity and thermal
75 conductivity) and hydraulic characteristics (empirical parameters of the soil water
76 retention curve and hydraulic conductivity) are usually obtained by fitting equations
77 (PTFs) to easily measured and widely available soil properties, such as sand, silt and
78 clay fractions, organic matter content, rock fragments and bulk density (Clapp and
79 Hornberger, 1978; Farouki, 1981; Vereecken et al., 2010; Dai et al., 2013). Soil albedos

80 are significantly correlated with the Munsell soil colour value (Post et al., 2000). For
81 some ESMs, the parameters derived by PTFs are used as direct input instead of being
82 calculated in the models.

83 2) Initial variables. The nutrient (C, N, P, K, S and so on.) amounts and the nutrients
84 associated parameters (pH, cation-exchange capacity, etc.) in soils can be used to
85 initialize the simulations. Generally, their initial values are assumed to be at steady state
86 by running the model over thousands of model years (i.e., spin-up) until there is no
87 change trend in pool sizes (McGuire et al., 1997; Thornton and Rosenbloom, 2005;
88 Doney et al., 2006; Luo et al., 2016). To initialize nutrient amounts using soil data
89 derived from observations as background fields could largely reduce the times of model
90 spin-up, and could avoid the possibility of a non-linear singularity evolution of the
91 model, which means that the models may have multiple equilibria and then provide a
92 better estimate of the true terrestrial nutrient state. The initial nutrient stocks settings
93 are major factors leading to model-to-model variation in simulation (Todd-Brown et al.,
94 2014).

95 3) Benchmark data. Soil data, as measurements, could serve as a reference for model
96 calibration, validation and comparison. Soil carbon stock is one of the soil properties
97 that is most frequently used as benchmark data (Todd-Brown et al., 2013). Other
98 nutrient stocks, such as nitrogen stock, can also be used as benchmark data if an ESM
99 simulated these properties.

100 Soil properties have great spatial heterogeneity both horizontally and vertically. As a
101 result, ESMs usually incorporate soil property maps (i.e., horizontal spatial distribution)
102 for multiply layers rather than a global constant or a single layer. ESMs, especially
103 LSMs, are evolving towards hyper-resolutions of 1 km or finer with more detailed
104 parameterization schemes to accommodate the land surface heterogeneity (Singh et al.,
105 2015; Ji et al., 2017). Therefore, spatially explicit soil data at high resolutions are
106 necessary to improve land surface representations and simulations. Because soil
107 properties are observed at individual locations, soil mapping or spatial prediction
108 models are needed to derive a 3D representation of the soil distribution. The traditional
109 method (i.e., the linkage method, also called the taxotransfer rule-based method)
110 involves linking soil profiles and soil mapping units on soil type maps, sometimes with
111 ancillary maps such as topography and land use (Batjes, 2003; FAO/IIASA/ISRIC/ISS-
112 CAS/JRC, 2012). In recent decades, various digital soil mapping technologies have
113 been proposed by finding the relationships between soil and environmental covariates
114 (usually remote sensing data), such as climate, topography, land use, geology and so on
115 (McBratney et al., 2003).

116 There are many challenges related to the application of soil datasets in ESMs. First, soil
117 datasets are usually not appropriately scaled or formatted for the use of ESMs and some
118 upscaling issues, which are the most frequently encountered, need to be addressed. The
119 soil datasets produced by the linkage methods are polygon-based and need to be
120 converted to fit the grid-based ESMs. This conversion can be performed by either the

121 subgrid method or spatial aggregation. The up-to-date soil data are provided at a
122 resolution of 1 km or finer, while the LSMs are mostly ran at a coarser resolution.
123 Therefore, soil data upscaling is necessary before it can be used by ESMs. Proper
124 upscaling methods need to be chosen carefully to minimize the uncertainty introduced
125 by these methods in the modelling results (Hoffmann and Christian Biernath, 2016;
126 Kuhnert et al., 2017). Second, all the current global soil datasets represent the average
127 state of the last decades, and the production of soil property maps in a time series is still
128 challenging. Soil landscape and pedogenic models are developed to simulate soil
129 formation processes and soil property changes, which can be incorporated into ESMs.
130 The prediction of changing soil properties can also be performed by digital soil mapping
131 using the changing climate and land use as covariates. Third, the uncertainty in the soil
132 properties can be estimated, and adaptive surrogate modelling based on statistical
133 regression and machine learning may be used to assess the uncertainty effects of soil
134 properties on ESMs (Gong et al., 2015; Li et al. 2018). Finally, the layer schemes of
135 soil data sets need to be converted for model use, and missing values for deeper soil
136 layers need to be filled.

137 This paper is organized into the following sections. In Sect. 2, we first introduce soil
138 datasets produced by the linkage method and digital soil mapping technology at global
139 and national scales, and then, we introduce the soil datasets that have already been
140 incorporated into ESMs, and we also present PTFs that are used in ESMs to estimate
141 soil hydraulic and thermal parameters. In Sect. 3, several global soil datasets are
142 compared and evaluated with a global soil profile database. In Sect. 4, two issues
143 regarding the model use of soil data are described and existing challenges related to the
144 application of soil datasets in ESMs are discussed. In Sect. 5, a summary and the
145 outlook of further improvements are provided.

146 **2 General methodology of deriving soil datasets for ESMs**

147 **2.1 Global and national soil datasets**

148 Two kinds of soil data are generated from soil surveys: maps (usually in the form of
149 polygon maps) representing the main soil types in landscape units and soil profiles with
150 soil property measurements which are considered to be representative of the main
151 component soils of the respective mapping units. ESMs usually require the spatial
152 distribution of soil properties (i.e., soil property maps) rather than information about
153 soil types. Two kinds of methods, i.e., the linkage method and the digital soil mapping
154 method, are used to derive the soil property maps.

155 Soil maps (the term soil map refers to soil type map in this paper) show the geographical
156 distribution of soil types, which are compiled under a certain soil classification system.
157 There are many soil mapping units (SMUs) in a soil map and an SMU is composed of
158 more than one component (i.e. soil type) in most cases. At the global level, there is only
159 one generally accepted global soil map, i.e., the FAO-UNESCO Soil Map of the World
160 (SMW) (FAO, 1971-1981). The SMW was made based on soil surveys conducted
161 between the 1930s and 1970s and technology that was available in the 1960s. Several
162 versions exist in the digital format (FAO, 1995, 2003b; Zöbler, 1986) and these

163 products are known to be outdated. The information on the initial SMW and DSMW
164 has since been updated for large sections of the world in the Harmonized World Soil
165 Database (HWSD) product (FAO/IIASA/ISRIC/ISS-CAS/JRC, 2012), which has
166 recently been revised in WISE30sec (Batjes, 2016).

167 At the regional and national levels, there are many soil maps based on either national
168 or international soil classifications. Some examples of major soil maps available in
169 digital formats are as follows: the Soil and Terrain Database (SOTER) databases (Van
170 Engelen and Dijkshoorn, 2012) for different regions, the European Soil Database (ESB,
171 2004), the 1: 1 million Soil Map of China (National Soil Survey Office, 1995), the U.S.
172 General Soil Map (GSM), the 1:1 million Soil Map of Canada (Soil Landscapes of
173 Canada Working Group, 2010) and the Australian Soil Resource Information System
174 (ASRIS) (Johnston et al., 2003).

175 Soil profiles are composed of multiple layers called soil horizons. For each horizon,
176 soil properties are observed (e.g., site data) or measured (e.g., pH, sand, silt, and clay
177 content). At the global level, several soil profile databases exist. Here, we discuss only
178 the two most comprehensive databases. The World Inventory of Soil Emission
179 Potentials (WISE) database was developed as a homogenized set of soil profiles (Batjes,
180 2008). The newest version (WISE 3.1) contains 10,253 soil profiles and 26 physical
181 and chemical properties. The soil profile database of the World Soil Information Service
182 (WoSIS) contains the most abundant profiles (about 118,400) from national and global
183 databases including most of the databases mentioned below (Batjes et al., 2017),
184 although only a selection of important soil properties (12) are included (Ribeiro et al.,
185 2018). Data from WoSIS have been standardized, with special attention to the
186 description and comparability of soil analytical methods worldwide. However, many
187 countries, although having a large collection of soil profile data, are not yet sharing
188 such data (Arrouays et al., 2017).

189 At the regional and national levels, there are many soil profile databases, usually with
190 soil classifications corresponding to the local soil maps, and here are some examples:
191 the USA National Cooperative Soil Survey Soil Characterization database
192 (<http://ncsslabdatamart.sc.egov.usda.gov/>), profiles from the USA National Soil
193 Information System (<http://soils.usda.gov/technical/nasis/>), Africa Soil Profiles
194 database (Leenaars, 2012), the ASRIS (Karssies, 2011), the Chinese National Soil
195 Profile database (Shangguan et al., 2013), soil profile archive from the Canadian Soil
196 Information System (MacDonald and Valentine, 1992), soil profiles from SOTER (Van
197 Engelen and Dijkshoorn, 2012), the soil profile analytical database for Europe (Hannam
198 et al., 2009), the Mexico soil profile database (Instituto Nacional de Estadística y
199 Geografía, 2016), and the Brazilian national soil profile database (Cooper et al., 2005).

200 The linkage method (called the taxotransfer rule-based method) involves linking soil
201 maps (with SMUs or soil polygons) and soil profiles (with soil properties) according to
202 taxonomy-based pedotransfer (taxotransfer in short, note that here, pedotransfer here
203 does not mean PTFs, which are a different thing) rules (Batjes, 2003). The criteria used

204 in the linkage could be one or many factors, such as following: soil class, soil texture
205 class, depth zone, topographic class, distance between soil polygons and soil profiles
206 (Shangguan et al., 2012). Each soil type is represented by one or a group of soil profiles
207 that meet the criteria, and usually, the median or mean value of a soil property is
208 assigned to the soil type. Because the linkage method assigned only one value or a
209 statistical distribution to a soil type in the soil polygons (usually a polygon contains
210 multiple soil types with their fractions), the intrapolygonal spatial variation is not
211 considered. At the global level, many databases were derived by the linkage method:
212 the FAO SMW with derived soil properties (FAO, 2003a), the Data and Information
213 System of International Geosphere-Biosphere Programme (IGBP-DIS) database
214 (Global Soil DataTask, 2000), the Soil and Terrain Database (Van Engelen and
215 Dijkshoorn, 2012) for multiply regions and countries, the ISRIC-WISE derived soil
216 property maps (Batjes, 2006), the HWSD (FAO/IIASA/ISRIC/ISS-CAS/JRC, 2012),
217 the Global Soil Dataset for Earth System Model (GSDE) (Shangguan et al., 2014) and
218 WISE30sec (Batjes, 2016). The three most recent databases are HWSD, GSDE and
219 WISE30sec. HWSD was built by combining the existing regional and national soil
220 information updates. GSDE, as an improvement of HWSD, incorporated more soil
221 maps and more soil profiles related to the soil maps, with more soil properties. GSDE
222 accomplished the linkage based on the local soil classification, which required no
223 correlation between classification systems and avoided the error brought by the
224 taxonomy reference. In addition, GSDE provides an estimation of eight layers to a depth
225 of 2.3 m, while HWSD provides an estimation of two layers to the depth of 1 m.
226 WISE30sec is another improvement of HWSD that incorporates more soil profiles with
227 seven layers up to 200 cm depth and with uncertainty estimated by the mean \pm standard
228 deviation. WISE30sec used the soil map from HWSD with minor corrections and
229 climate zone maps as categorical covariates. Many national and regional agencies
230 around the world have organized their soil surveys by linking soil maps and soil profiles,
231 including the USA State Soil Geographic Database (STATSGO2) (Soil Survey Staff,
232 2017), Soil Landscapes of Canada (Soil Landscapes of Canada Working Group, 2010),
233 the ASRIS (Johnston et al., 2003), the Soil-Geographic Database of Russia (Shoba et
234 al., 2008), the European Soil Database (ESB, 2004), and the China dataset of soil
235 properties (Shangguan et al., 2013).

236 Digital soil mapping (McBratney et al., 2003) is the creation and population of a
237 geographically referenced soil database, generated at a given resolution by using field
238 and laboratory observation methods coupled with environmental data through
239 quantitative relationships (<http://digitalsoilmapping.org/>). Usually, the soil datasets
240 derived by digital soil mapping provide grid-based spatially continuous estimation
241 while the soil datasets derived by the linkage method provide estimations with abrupt
242 changes at the boundaries of soil polygons. GlobalSoilMap is a global consortium that
243 aims to create global digital maps for key soil properties (Sanchez et al., 2009). This
244 global effort takes a bottom-up framework and produces the best available soil map at
245 a resolution of 3 arc sec (about 100 m) with 90% confidence in the predictions. Soil
246 properties will be provided for six soil layers (i.e., 0-5, 5-15, 15-30, 30-60, 60-100, and

247 100-200 cm). Many countries have produced soil maps following the GlobalSoilMap
248 specifications (Odgers et al., 2012; Viscarra Rossel et al., 2015; Mulder et al., 2016;
249 Ballabio et al., 2016; Ramcharan et al., 2018; Arrouays, 2018). The SoilGrids system
250 (<https://www.soilgrids.org>) is another global soil mapping project (Hengl et al., 2014;
251 Hengl et al., 2015; Hengl et al., 2017). The newest version (Hengl et al., 2017) at a
252 resolution of 250 m was produced by fitting an ensemble of machine learning methods
253 based on about 150,000 soil profiles and 158 soil covariates, which is currently the most
254 detailed estimation of global soil distribution. A third global soil mapping project is the
255 Global SOC (soil organic carbon) Map of the Global Soil Partnership, which focuses
256 on country-specific soil organic carbon estimates (Guevara et al., 2018).

257 Because soil property maps are products that are derived based on soil measurements
258 of soil profiles and spatial continuous covariates (including soil maps), it is necessary
259 to discuss the sources of uncertainty, spatial uncertainty estimation and accuracy
260 assessment of these derived data (the last two are different aspects of uncertainty
261 estimation). More attention should be given to this issue in ESM applications instead
262 of taking soil property maps as observations without error. There are various uncertainty
263 sources in the derivation of soil property maps, including uncertainty from soil maps,
264 soil measurements, soil-related covariates and the linkage method itself (Shangguan et
265 al., 2012; Batjes, 2016; Stoorvogel et al., 2017). The following uncertainties are not a
266 complete list of uncertainties, but the major uncertainties are listed. Uncertainties in
267 soil maps are major sources of global datasets derived by the linkage methods. For these
268 datasets, large sections of the world are incorporated into the coarse FAO SMW map,
269 and the purity of soil maps (referring to the following website for the definition:
270 [https://esdac.jrc.ec.europa.eu/ESDB_Archive/ESDBv2/esdb/sgdbe/metadata/purity_m
271 aps/purity.htm](https://esdac.jrc.ec.europa.eu/ESDB_Archive/ESDBv2/esdb/sgdbe/metadata/purity_maps/purity.htm)) is likely to be around 50 to 65% (Landon, 1991). Another important
272 source of uncertainty is the limited comparability of different analytical methods for a
273 given soil property when using soil profiles from various sources. A weak correlation
274 or even a negative correlation was found between different analytical methods,
275 although a strong positive correlation was revealed in most cases (McLellan et al. 2013).
276 Both datasets of the linkage method and those by digital soil mapping are subject to this
277 uncertainty. Although there are no straightforward mechanisms to harmonize the data,
278 efforts have been undertaken to address this issue and provide quality assessment
279 (Batjes, 2017; Pillar 5 Working Group, 2017). Another source of uncertainty comes
280 from the geographic and taxonomic distribution of soil profiles, especially for the
281 under-represented areas and soils (Batjes, 2016). The fourth source of uncertainty is
282 from the linkage method itself. The linkage method does not represent the intra-polygon
283 spatial variation and usually does not explicitly consider soil-related covariates like
284 digital soil mapping, although there are cases where climate and topography are
285 considered; and Stoorvogel et al. (2017) proposed a methodology to incorporate
286 landscape properties in the linkage method. Finally, uncertainty from the covariates is
287 minor because spatial prediction models such as machine learning in digital soil
288 mapping can reduce its influences (Hengl et al., 2014), although a more comprehensive
289 list of covariates with higher resolution and accuracy will improve the predicted soil

290 property maps. Spatial uncertainty is estimated by different methods for the linkage
291 method and digital soil mapping methods. For the linkage method, statistics such as
292 standard deviation and percentiles can be used for the spatial uncertainty estimation,
293 and these statistics are calculated for the population of soil profiles linked to a soil type
294 or a land unit (Batjes, 2016). This estimation has some limitations because soil profiles
295 are not taken probabilistically but based on their availability, especially for the global
296 soil datasets. Uncertainty will be underestimated when the sample size is not large
297 enough to represent a soil type. For digital soil mapping, spatial uncertainty could be
298 estimated by methods such as geostatistical methods and quantile regression forest
299 (Vaysse and Lagacherie, 2017), which make sense of the statistics. The accuracy of the
300 soil datasets derived by digital soil mapping is estimated by independent validation or
301 cross-validation. However, this estimation is not trivial for those data derived by the
302 linkage method due to the global scale, the support of the data and independent data
303 (Stoorvogel et al., 2017), and most of these maps are validated by statistics such as the
304 mean error and coefficient of determination. Instead, some datasets, including WISE
305 and GSDE, use indicators such as the linkage level of soil class and sample size to offer
306 quality control information (Shangguan et al. 2014; Batjes, 2016). A simple way to
307 compare the accuracy of using datasets with both methods may be to use a global soil
308 profile database as a validation dataset, though quite a number of these profiles were
309 used when deriving these datasets and questions will be raised. We evaluated several
310 global soil property maps in Sect. 3.

311 **2.2 Soil dataset incorporated in ESMs**

312 Table 1 shows ESMs (specifically, their LSMs) and their input soil datasets. The ESMs
313 in Table 1 cover the CMIP5 (Coupled Model Intercomparison Project) list except those
314 without information about the soil dataset inputs. LSMs are key tools to predict the
315 dynamics of land surfaces under climate change and land use. Five datasets are widely
316 used, i.e., the datasets by Wilson and Henderson-Sellers (1985), Zöbner (1986), Webb
317 et al. (1993), Reynolds et al. (2000), Global Soil Data Task (2000), and Miller and
318 White (1998). Except for GSDE, HWSD and STATSGO (Miller and White, 1998) for
319 the USA in Table 1, these datasets were derived from the SMW (note that large sections
320 of GSDE and HWSD still used this map as a base map because there are no available
321 regional or national maps) (FAO, 1971-1981) and limited soil profile data (no more
322 than 5,800 profiles), which gained popularity because of its simplicity and ease of use.
323 However, these datasets are outdated and should no longer be used because much better
324 soil information, as introduced in Sect. 2.1, can be incorporated (Sanchez et al., 2009;
325 FAO/IIASA/ISRIC/ISS-CAS/JRC, 2012).

326 In recent years, efforts have been made to improve the soil data condition in ESMs. The
327 Land-Atmosphere Interaction Research Group at Sun Yat-sen University (formerly at
328 Beijing Normal University) has put much effort into this topic. Shangguan et al. (2012,
329 2013) developed a China soil property dataset for land surface modelling based on
330 8,979 soil profiles and the Soil Map of China using the linkage method. Dai et al. (2013)
331 derived soil hydraulic parameters using PTFs based on the soil properties by Shangguan
332 et al. (2013). Shangguan et al. (2014) further developed a comprehensive global dataset

333 for ESMs. The above soil datasets were widely used in the ESMs. Soil properties from
334 these soil datasets, including soil texture fraction, organic carbon, bulk density and
335 derived soil hydraulic parameters, were implemented in the Common Land Model
336 Version 2014 (CoLM2014, <http://land.sysu.edu.cn/>). Li et al. (2017) showed that
337 CoLM2014 was more stable than the previous version and had comparable performance
338 to that of CLM4.5, which may be partially attributed to the new soil parameters being
339 used as input. Wu et al. (2014) showed that soil moisture values are closer to the
340 observations when simulated by CLM3.5 with the China dataset than those simulated
341 with FAO. Zheng and Yang (2016) estimated the effects of soil texture datasets from
342 FAO and BNU based on regional terrestrial water cycle simulations with the Noah-MP
343 land surface model. Tian et al. (2012) used the China soil texture data in a land surface
344 model (GWSiB) coupled with a groundwater model. Lei et al. (2014) used the China
345 soil texture data in CLM to estimate the impacts of climate change and vegetation
346 dynamics on runoff in the mountainous region of the Haihe River basin. Zhou et al.
347 (2015) estimated age-dependent forest carbon sinks with a terrestrial ecosystem model
348 utilizing China soil carbon data. Dy and Fung (2016) updated the soil data for the
349 Weather Research and Forecasting model (WRF).

350 Researchers have also put efforts into updating ESMs with other soil data. Lawrence
351 and Chase (2007) used MODIS data to derive soil reflectance, which was used as a soil
352 colour parameter in the Community Land Model 3.0 (CLM). De Lannoy et al. (2014)
353 updated the NASA Catchment land surface model with soil texture and organic matter
354 data from HWSD and STATSGO2. Livneh et al. (2015) evaluated the influence of soil
355 textural properties on hydrologic fluxes by comparing the FAO data and STATSGO2.
356 Folberth et al. (2016) evaluated the impact of soil input data on yield estimates in a
357 globally gridded crop model. Slevin et al. (2017) utilized the HWSD to simulate global
358 gross primary productivity in the JULES land surface model. Trinh et al. (2018)
359 proposed an approach that can assimilate coarse global soil data by finer land use and
360 coverage datasets, which improved the performance of hydrologic modelling at the
361 watershed scale. Kearney and Maino (2018) incorporated the new generation of soil
362 data produced by the digital soil mapping method into a climate model and found that
363 compared to the old soil information, the soil moisture simulation was improved at a
364 fine spatial and temporal resolution over Australia. A dataset of globally gridded
365 hydrologic soil groups (HYSOGs250m) were developed based on soil texture and depth
366 to bedrock of SoilGrids (Hengl et al., 2017) and groundwater table depth (Fan et al.,
367 2013) for curve-number based runoff modelling of the U.S. Department of Agriculture
368 (Ross et al., 2018).

369 Except for soil properties, the estimation of underground boundaries, including the
370 groundwater table depth, the depth to bedrock (DTB) and depth to regolith and its
371 implementation in ESMs is also a new focus. Fan et al. (2013) compiled global
372 observations of water table depth and inferred the global patterns using a groundwater
373 model. Pelletier et al. (2016) developed a global DTB dataset using process-based
374 models for upland and an empirical model for lowland. This dataset was implemented
375 in CLM4.5, and there were significant influences on the water and energy simulations

376 compared to the default constant depth (Brunke et al., 2015). Shangguan et al. (2017)
377 developed a global DTB by digital soil mapping based on about 1.7 million
378 observations from soil profiles and water wells, which has a much higher accuracy than
379 the dataset by Pelletier et al. (2016). Vrettas and Fung (2016) showed that weathered
380 bedrock stores a significant fraction (more than 30%) of the total water despite its low
381 porosity. Jordan et al. (2018) estimated the global permeability of the unconsolidated
382 and consolidated earth for groundwater modelling. However, due to the lack of data, an
383 accurate global estimation of depth to regolith is not feasible. Caution should be used
384 when employing the so-called soil depth products in ESMs. Soil depth maps are usually
385 estimated based on observations from soil surveys, and soil depth (or depth to the R
386 horizon) is assumed to be equal to DTB. However, these observations are usually less
387 than 2 metres and usually do not reach the DTB (Shangguan et al., 2017). Thus, soil
388 depth maps based on only soil profiles are significantly underestimated (one order of
389 magnitude lower) compared to the actual DTB and should not be taken as the lower
390 boundary of ESMs.

391 **2.3 Estimating secondary parameters using PTFs**

392 Earth system modellers have employed different PTFs to estimate soil hydraulic
393 parameters (SHP), soil thermal parameters (STP), and biogeochemical parameters
394 (Looy et al., 2017; Dai et al., 2013) or used these parameters as model inputs. Nearly
395 all ESMs incorporated SHPs and STPs estimated by PTFs but not biogeochemical
396 parameters. PTFs are the empirical, predictive functions that account for the
397 relationships between certain soil properties (e.g., hydraulic conductivity) and more
398 easily obtainable soil properties (e.g. sand, silt, clay and organic carbon content). Direct
399 measurement of these parameters is difficult, expensive and in most cases impractical
400 for obtaining sufficient samples to reflect spatial variation. Thus, most soil databases
401 do not contain these parameters. PTFs provide an alternative means of estimating these
402 parameters. In ESMs, SHPs and STPs are usually derived using simple PTFs, using
403 only soil texture data as the input. As more soil properties become globally available,
404 including gravel, soil organic matter and bulk density, more sophisticated PTFs that use
405 additional soil properties can be employed in ESMs.

406 PTFs can be expressed as either numerical equations or by machine learning
407 methodology which is more flexible for simulating the highly nonlinear relationship in
408 analysed data. PTFs can also be developed based on soil processes. Most researches
409 have not indicated where the PTFs can potentially be used, and the accuracy of a PTF
410 outside of its development dataset is essentially unknown (McBratney et al., 2011).
411 PTFs are generally not portable from one region to another (i.e. locally or regionally
412 validated). Therefore, PTFs should never be considered as an ultimate source of
413 parameters in soil modelling. Looy et al. (2017) reviewed PTFs extensively in earth
414 system science and emphasized that PTF development must go hand in hand with
415 suitable extrapolation and upscaling techniques such that the PTFs correctly represent
416 the spatial heterogeneity of soils in ESMs. Although the PTFs were evaluated, it is
417 unclear which set of PTFs are the best for global applications. Due to these limitations,
418 a better way to estimate these parameters may be to use an ensemble of PTFs, which

419 can provide the parameter variability. Dai et al. (2013) derived a global soil hydraulic
420 parameter database using the ensemble method. Selection of PTFs was carried out
421 based on the following rules, including a consistent physical definition, adequately
422 large training sample and positive evaluations that are comparable with other PTFs. The
423 selected PTFs not only included those in equations but also machine learning PTFs. As
424 a result, the modellers could use these parameters as inputs instead of calculating them
425 in ESMs every time the model was run.

426 New generation soil information has already been utilized to derive SHPs and STPs in
427 some studies. Montzka et al. (2017) produced a global map of SHPs at a 0.25°
428 resolution based on the SoilGrids 1 km dataset. Tóth et al. (2017) calculated SHPs for
429 Europe with EU-HYDI PTFs (Tóth et al., 2015) based on the SoilGrids 250 m. Wu et
430 al. (2018) used an integrated approach that ensembles PTFs to map the field capacity
431 of China based on multi-source soil datasets.

432 The PTF performance in ESMs has been evaluated in many studies, although PTFs
433 have not been fully exploited and integrated into ESMs (Looy et al., 2017). Some
434 examples are as follows. Chen et al. (2012) incorporated soil organic matter to estimate
435 soil porosity and thermal parameters for use in LSMs. Zhao et al. (2018a) evaluated
436 PTFs performance to estimate SHPs and STPs for land surface modelling over the
437 Tibetan Plateau. Zheng et al. (2018) developed PTFs to estimate the soil optical
438 parameters to derive soil albedo for the Tibetan Plateau, and the PTFs that were
439 incorporated into an eco-hydrological model improved the model simulation of a
440 surface energy budget. Looy et al. (2017) envisaged two possible approaches to
441 improve parameterization of ESMs by PTFs. One approach is to replace constant
442 coefficients in current ESMs that have spatially distributed values with PTFs. The other
443 approach is to develop spatially exploitable PTFs to parameterize specific processes
444 using knowledge of environmental controls and variations in soil properties.

445 **3 Comparison of available global soil datasets**

446 For the convenience of ESMs' application, we compared several available soil datasets
447 and evaluated them with soil profiles from WoSIS for some of the key variables (sand,
448 clay content, organic carbon, coarse fragment and bulk density) used in ESMs. In
449 addition to the most recent developed soil datasets, we also included one old data set
450 (i.e., IGBP) used in ESMs for the evaluation. It is not necessary to compare all the old
451 data sets because they are based on similar, limited and outdated source data as
452 described in Sect. 2.2. These datasets have coarser resolutions (Table 1) than the newly
453 developed soil datasets (Table 2).

454 We present basic descriptions of the new soil datasets in Table 2 and 3. As described in
455 Sect. 2.1, four available global soil datasets, i.e., HWSD, GSDE, WISE30sec and
456 SoilGrids, have been developed in the last several years (Table 2). These soil datasets
457 are selected to be shown here because they have global coverage with key variables
458 used by ESMs and were developed with relatively good data sources in recent years;
459 these data are also freely available. Old versions of these datasets are not shown here.

460 Table 3 shows the available soil properties of these soil datasets. Except for WISE30sec,
461 none of these databases contain spatial uncertainty estimations. The explained soil
462 property variance in SoilGrids is between 56% and 83%, while the other datasets do
463 not offer quantitative accuracy assessments. GSDE has the largest number of soil
464 properties, while SoilGrids currently contains ten primary soil properties defined by the
465 GlobalSoilMap consortium.

466 The accuracy of the newly developed soil datasets (SoilGrids, GSDE and HWSD) and
467 an old dataset (IGBP) are evaluated for five key variables using 94,441 soil profiles
468 from WoSIS (Table 4), though quite a number of the WoSIS soil profiles were
469 considered in the compilation of these datasets which means that this evaluation is not
470 independent validation. We used four statistics in the evaluation, including mean error
471 (ME), root mean squared error (RMSE), coefficient of variation (CV) and coefficient
472 of determination (R^2). All soil datasets are evaluated for topsoil (0-30 cm) and subsoil
473 (30-100 cm). The layer schemes of soil datasets are different (Table 1) and were
474 converted to the two layers. Soil datasets are high in resolution and were converted to
475 a resolution of 10 km by averaging. All datasets have relatively small ME. In general,
476 SoilGrids have much better accuracy than the other three due to RMSE, CV and R^2 ,
477 and GSDE ranks the second, followed by IGBP and HWSD. However, IGBP is slightly
478 better than GSDE for bulk density and organic carbon content of topsoil. Notably, only
479 the IGBP does not contain coarse fragments, which is needed when calculating soil
480 carbon stocks. We did not evaluate the WISE30sec here to save time in data processing,
481 because previous evaluation using WoSIS showed that WISE30sec had slightly better
482 accuracy than HWSD
483 (<https://github.com/thengl/SoilGrids250m/tree/master/grids/HWSD>). This evaluation
484 has some limitations. First, the datasets developed by the linkage method, which give
485 the mean value of a SMU, resulted in an abrupt change between the boundaries of soil
486 polygons whereas the datasets developed by digital soil mapping simulated the soil as
487 a continuum with a spatial continuous change in soil properties; thus, these datasets
488 may not be comparable. Second, the original resolutions of soil datasets are different,
489 which means that maps with higher resolutions provide more spatial details, and we
490 should judge the map quality by not only the accuracy assessment but also by the
491 resolution. As a result, datasets with higher resolutions (i.e. HWSD, WISE30sec and
492 GSDE) are preferred to those with lower resolutions (i.e., IGBP) because the higher
493 resolution datasets have similar accuracy, especially when the LSMs are run at a high
494 resolution, such as 1 km. Third, the vertical variation is better represented by SoilGrids,
495 GSDE and WISE30sec with more than 2 layers and a depth of over 2m (Table 2), which
496 will provide more useful information for ESMs, especially when they model deeper
497 soils with multiple layers.

498 The new generation soil dataset produced by the digital soil mapping method gave a
499 very different distribution of soil properties from those produced by the linkage method.
500 Figure 1 shows the soil sand and clay fractions at the surface 0-30 cm layer from
501 SoilGrids, IGBP and GSDE. Figure 2 shows the SOC and bulk density at the surface 0-
502 30 cm layer from SoilGrids, IGBP and GSDE. Significant differences are visible in

503 these datasets. This difference will lead to different modelling results in ESMs. Tifafi
504 et al. (2018) found that the global SOC stocks down to a depth of 1 m is 3,400 Pg when
505 estimated by SoilGrids and 2500 according to HWSD, and the estimates by SoilGrids
506 are closer to the actual observations, although all datasets underestimated the soil
507 carbon stocks. Figure 1 of Tifafi et al. (2018) shows the global distribution of soil
508 carbon stocks by SoilGrids and HWSD.

509 In general, SoilGrids is preferred for ESMs' application because it currently has the
510 highest accuracy and resolution. When soil properties are not available in SoilGrids,
511 WISE30sec and GSDE offer alternative options. However, model sensitivity
512 simulations need to be performed to investigate the effects of different soil datasets on
513 ESMs in future studies.

514 **4 Soil data usage in ESMs and existing challenges**

515 **4.1 Model use of soil data derived by the linkage method**

516 Soil data by the linkage method are derived for each SMU or land unit and thus are
517 polygon-based, while ESMs are usually grid-based. However, soil data derived by
518 digital soil mapping are grid-based. Therefore, the compatibility between soil data
519 derived by the linkage method and ESMs must be addressed. In the soil map, a SMU is
520 composed of more than one component soil unit in most cases, and thus, a one-to-many
521 relationship exists between the SMU and profile attributes of the respective soil units.
522 This condition makes representing the attributes characterizing an SMU a nontrivial
523 task. To keep the whole soil variation of in an SMU, it is best to use the subgrid method
524 in ESMs (Oleson et al., 2010), i.e. aggregate values of soil properties, and provide the
525 area percentage of each value. This will bring about the problem of mapping the soil
526 subgrids with land cover (or plant function type) subgrids. A possible solution is to
527 classify the soil according to the soil properties and obtain a number of defined soil
528 classes (n classes) such as land cover types (m classes), overlay the defined soil classes
529 with land cover types and obtain n by m combinations assuming the soil classes and
530 land cover types are independent. However, this will increase the computing time and
531 complexity of the ESMs' structures, which requires implementation the soil processes
532 over each subgrid soil column within a grid instead of the entire model grid.

533 Usually, the compatibility issue is addressed by converting the SMU-based soil data to
534 grid data using spatial aggregation. The ESMs uses grid data as input, and each grid
535 cell has one unique value of a soil property. Three spatial aggregation methods were
536 proposed to aggregate compositional attributes in an SMU to a representative value
537 (Batjes, 2006; Shangguan et al., 2014). The area-weighting method (method A) obtains
538 the area-weighting of soil attributes. The dominant type method (method D) obtains the
539 soil attribute of the dominant type. The dominant binned method (method B) classifies
540 the soil attributes into several preselected classes and obtains the dominant class. All
541 three methods can be applied to quantitative data, while method D and method B can
542 be applied to categorical data. The advantages and disadvantages of these methods have
543 been discussed (Batjes, 2006; Shangguan et al., 2014). The choice should be made
544 according to the specific applications (Hoffmann et al., 2016). Method B provides

545 binned classes, which are not convenient for modelling, although method B is
546 considered more appropriate to represent a grid cell. Method A maintains mass
547 conservation, which can meet most model application demands. However, method A
548 may be misleading in cases where extreme values appeared in an SMU. For the linkage
549 method, the uncertainty is usually estimated by obtaining the 5 and 95 percentile soil
550 properties (or other statistics) of the soil profiles that are linked to an SMU. Because
551 the frequency distribution of the soil properties within a SMU is usually not a normal
552 distribution or any other typical statistical distribution, the application of statistics such
553 as standard deviation to model use is not proper. This means that the uncertainty in the
554 soil dataset derived by the linkage method cannot be incorporated into ESMS in a
555 straightforward way, and technology such as bootstrap may be more suitable than
556 methods that make assumptions on regarding the distribution.

557 The basic soil properties are often used to derive the secondary parameters, including
558 SHPs and STPs by PTFs and soil carbon stock or other nutrient stocks by certain
559 equations (Shangguan et al., 2014). This procedure could be performed either before or
560 after the aggregation (referred to here as “aggregating after” and “aggregating first”).
561 Because the relationship between the soil basic properties and the derived soil
562 parameters is usually nonlinear, the “aggregating first” method should be used. This
563 was also proven by case studies (Romanowicz et al., 2005; Shangguan et al., 2014).
564 However, some researchers have used the “aggregating after” method to produce
565 misleading results (Hiederer and Köchy, 2012).

566 The aggregation smooths the variation in the soil properties between soil components
567 within a given SMU (Odgers et al., 2012). To avoid aggregation, the spatial
568 disaggregation of soil type maps can be used to determine the location of the SMU
569 components, although the location error may be high in some cases (Thompson et al.,
570 2010; Stoorvogel et al., 2017). This method depends on the high density of soil profiles
571 to establish soil and landscape relationships. Folberth et al. (2016) showed that the
572 correct spatial allocation of the soil type to the present cropland was very important in
573 global crop yield simulations. Currently, aggregation is still the practical method to use
574 at the global scale due to lack of data.

575 **4.2 Upscaling detailed soil data for model use**

576 The updated soil datasets derived by both the linkage method and digital soil mapping
577 are usually at a resolution from 1 km to 100 m, and upscaling or aggregation is required
578 to derive lower resolution datasets for model use. The aggregation methods mentioned
579 above can be used. Moreover, there are many upscaling methods such as the window
580 median, variability-weighted methods (Wang et al., 2004), variogram method (Oz et al.,
581 2002), fractal theory (Quattrochi et al., 2001) and the Miller-Miller scaling approach
582 (Montzka et al., 2017). However, few studies have been devoted to determining the
583 upscaling methods that are suitable for soil data. A preliminary effort was made by
584 Shangguan (2014). Five upscaling methods were compared, including the window
585 average, window median, window modal, arithmetic average variability-weighted
586 method and bilinear interpolation method. Differences between aggregation methods

587 varied from 10% to 100% for different parameters. The upscaling methods affected the
588 data derived by the linkage method more than the data derived by digital soil mapping.
589 The window average, window median and arithmetic average variability-weighted
590 method performed similar in upscaling. The RMSE increased rapidly when the window
591 size was less than 40 pixels. Similar to the aggregation of SMUs, the “aggregating first”
592 method is recommended when secondary soil parameters are derived. Again, an
593 alternative to avoid the aggregation into one single value for a grid cell is to use the
594 subgrid method in ESMs.

595 The upscaling effect of soil data on the model simulation has been investigated in
596 previous studies with controversial conclusions. For example, Melton et al. (2017) used
597 two linked algorithms to provide tiles of representative soil textures for subgrids in a
598 terrestrial ecosystem model and found that the model is relatively insensitive to subgrid
599 soil textures compared to a simple grid-mean soil texture at a global scale. However,
600 the treatment without soil subgrid structure in JULES resulted in soil moisture
601 dependent anomalies in simulated carbon flux (Park et al., 2018). Further researches
602 are necessary to investigate the upscaling effect on models.

603 **4.3 The changing soil properties**

604 There are no global soil property maps in the time-series because we do not have
605 enough available data. In all global soil property maps, all available soil observations
606 in recent decades have been used in the development of soil property maps without
607 considering the changing environment. Therefore, these datasets should be considered
608 as an average state. The critical issue for mapping global soil properties in a time series
609 is to establish a soil profile database with time stamps and then divide them into two or
610 more groups of different periods such as the 1950s-1970s. This is still quite challenging
611 at the global scale because the spatial coverage of soil profiles is quite uneven for
612 different periods and the sample size may not be adequately large to derive maps with
613 satisfactory accuracy.

614 Soil properties are changing, but we are now usually considering them to be static in
615 ESMs. As some ESMs already simulate the soil carbon, this may be considered in PTFs
616 used to estimate soil hydraulic and thermal parameters. Other soil properties affecting
617 soil hydraulic and thermal parameters include soil texture, bulk density, and soil
618 structure, but the change is relatively slow. The effect of environmental change on soil
619 properties is the topic of the quantitative modelling of soil forming processes, i.e., soil
620 landscape and pedogenic models (Gessler et al., 1995; Minasny et al., 2008). If we need
621 to simulate the change in soil properties, a coupling of ESMs and soil landscape and
622 pedogenic models will be needed. Otherwise, we need to predict the soil properties in
623 the future using soil landscape and pedogenic models, which are small scale with high
624 uncertainty. The prediction of changing soil properties may also be performed by digital
625 soil mapping taken the changing (especially for the future) climate and land use as
626 covariates, which may be easier and more feasible than dynamic models.

627 **4.4 Incorporating the uncertainty of soil data in ESMs**

628 Incorporating the uncertainty of soil data in ESMs is increasing challenging. Except for
629 WISE30sec, all the current global soil datasets do not have a corresponding uncertainty
630 map for a soil property. However, the spatial uncertainty can be estimated by the
631 methods mentioned in Sect. 2.1, and soil datasets with uncertainty maps will be made
632 available sooner or later. It is too expensive to run multiply ESM simulations that
633 combine the upper and lower bounds in all possible combinations to quantify the effect
634 of soil data uncertainty on ESMs. Instead, adaptive surrogate modelling based on
635 statistical regression and machine learning can be used to emulate the responses of
636 ESMs to the variation of soil properties at each location, which uses much less
637 computing time and proves to be effective and efficient (Gong et al., 2015; Li et al.
638 2018).

639 **4.5 Layer schemes and lack of deep layer soil data**

640 The layer scheme of a soil data set needs to be converted to that of ESMs for model use.
641 A simple method for this conversion is the depth weighting method. When a more
642 accurate conversion is needed, the equal-area quadratic smoothing spline functions can
643 be used, which is advantageous in predicting the depth function of soil properties
644 (Bishop et al., 1999). Mass conservation for a soil property of a layer is guaranteed by
645 this method under the assumption of a continuous vertical variation in soil properties.
646 This method may produce some negative values that should be set to zero.

647 The depth of soil observations in the soil survey is usually less than 2 m and thus results
648 in missing values for the deep layers of ESMs. For the lack of deep soil data, there is
649 no good solution other than extrapolating the values based on the observations of
650 shallower layers, which will lead to higher uncertainty of soil properties for deep layers.
651 The extrapolation can be performed by the abovementioned spline method or simply
652 by assigning the soil properties of the last layer to the rest of the deeper soil layers. The
653 DTB map (Shangguan et al., 2017) can be utilized to define the low boundary of soil
654 layers, and a default set of thermal and hydraulic characteristics can be assigned for
655 bedrocks.

656 **5 Summary and outlook**

657 In this paper, the status of soil datasets and their usage in ESMs is reviewed. Soil
658 physical and chemical properties serve as model parameters, initial variables or
659 benchmark datasets in ESMs. Soil profiles, soil maps and soil datasets derived by the
660 linkage method and digital soil mapping are reviewed at national, regional and global
661 levels. The soil datasets derived by digital soil mapping are considered to provide a
662 more realistic estimation of soils than those derived by the linkage method, because
663 digital soil mapping provides spatially continuous estimations of soil properties using
664 spatial prediction models with various soil-related covariates. Due to the evaluation of
665 soil datasets by WoSIS, SoilGrids have the most accurate estimation of soil properties.
666 However, other soil datasets, including GSDE and WISE30sec, can be considered as
667 compensation and they provide more soil properties.

668 The popular soil datasets used in ESMS are outdated and there are updated soil datasets
669 available. In recent years, efforts have been made to update the soil data in ESMS. The
670 effects of updated soil properties which are used to estimate soil hydraulic and thermal
671 parameters, were evaluated. Other major updates include soil reflectance, ground water
672 tables and DTB.

673 PTFs are employed to estimate secondary soil parameters, including soil hydraulic and
674 thermal parameters, and biogeochemical parameters. PTFs can take more soil
675 properties (i.e., SOC, bulk density and so on.) as input in addition to soil texture data.
676 An ensemble of PTFs may be more suitable to provide secondary soil parameters as
677 direct input to ESMS, because the ensemble method has a number of benefits and
678 potential over a single PTF (Looy et al., 2017).

679 Soil data derived by the linkage methods and high-resolution data can be aggregated by
680 different methods to be use in ESMS. The aggregation should be performed after the
681 secondary parameters are estimated. However, the aggregation will omit the soil
682 property variation. To avoid aggregation, the subgrid method in ESMS is an alternative
683 that increases the model complexity. The effect of different upscaling methods on the
684 performance of ESMS needs to be further investigated.

685 Because digital soil mapping has many advantages compared to the traditional linkage
686 method, especially in representing spatial heterogeneity and quantifying uncertainty in
687 the predictions, the new generation soil datasets derived by digital soil mapping need
688 to be tested in ESMS, and some regional studies have shown that these datasets provide
689 better modelling results than products by the linkage method (Kearney and Maino, 2018;
690 Trinh et al., 2018). Moreover, many studies from digital soil mapping have identified
691 that soil maps are not very important for predicting soil properties and are usually not
692 used as a covariate in most studies (e.g., Hengl et al., 2014; Viscarra Rossel et al., 2015;
693 Arrouays et al., 2018). However, the linkage method usually considers the soil map to
694 be a base map, which essentially affects the accuracy of the derived soil property maps,
695 especially for areas without detailed soil maps. As a data-driven method, digital soil
696 mapping requires soil profile measurements and environmental covariates (in which the
697 importance of soil maps is low), and by including more of these data in mapping will
698 improve the global predictions (Hengl et al., 2017). More quality assessed data,
699 analysed according to comparable analytical methods, are needed to support such
700 efforts. The soil data harmonization is undertaken by the work of GSP Pillar 5 (Pillar 5
701 Working Group, 2017) and WoSIS (Batjes et al., 2017). Data derived from proximal
702 sensing, although with higher uncertainty than traditional soil measurements, can be
703 used in soil mapping (England and Viscarra Rossel, 2018). To avoid spatial
704 extrapolation, soil profiles should have good geographical coverage. The temporal
705 variation in global soil is quite challenging due to a lack of data. Soil image fusion is
706 also needed to merge the local and global soil maps, and this fusion considers these
707 maps as soil variation components for ensemble predictions (Hengl et al., 2017). It may
708 take years before a system for automated soil image fusion is fully functional in an
709 operational system for global soil data fusion. Mapping the soil depth and DTB

710 separately at the global level also remains challenging due to a lack of data and the
711 understanding of relevant processes. Uncertainty estimation, especially spatial
712 uncertainty estimation should be included in the soil datasets developed in the future.
713 However, incorporating the spatial uncertainty of the soil properties in ESMS is still
714 challenging due to the cost, and an alternative may be to use adaptive surrogate
715 modelling.

716 The gap is large between the amount of data that has been obtained in surveys and the
717 amount of data freely available. The soil profiles included in global soil databases such
718 as WoSIS comprise a very small fraction of the soil pits dug by human beings. For
719 example, there are more than 100,000 soil profiles from the second national soil survey
720 of China (Zhang et al., 2010) and no more than 9,000 were used to produce the national
721 soil property maps that are freely available (Shangguan et al., 2013). In the last century,
722 national soil surveys have been widely accomplished, primarily for agriculture purpose.
723 However, most of these legacy data are not digitalized and they are usually not made
724 available to the science community even if digitalized. Obtaining these hidden soil data
725 will require some mechanism such as government mandated regulations and money
726 investments to make these data available (Pillar four Working Group, 2014; Pillar 5
727 Working Group, 2017). Arrouays et al. (2017) reported that about 800,000 soil profiles
728 have been obtained from the selected countries, although most of these are not yet freely
729 available to the international community. In addition, investments in new soil samplings
730 should be made, especially in the under-represented areas. A good example is the U.S.,
731 which has the most abundant soil data freely available
732 (<http://ncsslabdatamart.sc.egov.usda.gov/>) similar to many other data. Censored
733 information produces censored maps and so on. If the hidden data could be made
734 available in any way, science and the whole human being will be promoted. A true big
735 data era is waiting for us. The data compatibility of different analysis methods and
736 different description protocols including soil classifications is also an important issue
737 and data harmonization is necessary when the data are made available to the public.

738 **Data availability.** The underlying research data used can be accessed as follows:
739 HWSD, GSDE, WISE30sec, SoilGrids and WoSIS are freely available at
740 <http://www.iiasa.ac.at/web/home/research/researchPrograms/water/HWSD.html>,
741 <http://globalchange.bnu.edu.cn/research/data>, [https://www.isric.org/explore/wise-](https://www.isric.org/explore/wise-databases)
742 [databases, http://www.soilgrids.org](http://www.soilgrids.org) and <https://www.isric.org> respectively.

743
744 **Author contributions.** YD planned and led the work and wrote part of the paper, WS
745 did the analysis and wrote most content of the work, DW, NW, QX, HY, SZ, SL, XL
746 and FY suggested the study.

747
748 **Competing interests.** The authors declare that they have no conflict of interest.
749

750 **Acknowledgements.** We thank two anonymous referees and the editors for their
751 comments who helped us improving the paper much. This work was supported by the
752 National Key Research and Development Program of China under grants

753 2017YFA0604303 and 2016YFB0200801 and the Natural Science Foundation of
754 China (under grants 41575072, 41730962 and U1811464).

755 **References**

756 Arora, V.K., Boer, G.J., Christian, J.R., Curry, C.L., Denman, K.L., Zahariev, K.,
757 Flato, G.M., Scinocca, J.F., Merryfield, W.J. and Lee, W.G.: The Effect of Terrestrial
758 Photosynthesis Down Regulation on the Twentieth-Century Carbon Budget Simulated
759 with the CCCma Earth System Model, *Journal of Climate* 22, 6066-6088, 2009.

760 Arrouays, D., Leenaars, J. G. B., Richer-de-Forges, A. C., Adhikari, K., Ballabio, C.,
761 Greve, M., Grundy, M., Guerrero, E., Hempel, J., Hengl, T., Heuvelink, G., Batjes, N.,
762 Carvalho, E., Hartemink, A., Hewitt, A., Hong, S.-Y., Krasilnikov, P., Lagacherie, P.,
763 Lelyk, G., Libohova, Z., Lilly, A., McBratney, A., McKenzie, N., Vasquez, G. M.,
764 Mulder, V. L., Minasny, B., Montanarella, L., Odeh, I., Padarian, J., Poggio, L.,
765 Roudier, P., Saby, N., Savin, I., Searle, R., Solbovoy, V., Thompson, J., Smith, S.,
766 Sulaeman, Y., Vintila, R., Rossel, R. V., Wilson, P., Zhang, G.-L., Swerts, M., Oorts,
767 K., Karklins, A., Feng, L., Ibelles Navarro, A. R., Levin, A., Laktionova, T.,
768 Dell'Acqua, M., Suvannang, N., Ruam, W., Prasad, J., Patil, N., Husnjak, S., Pásztor,
769 L., Okx, J., Hallett, S., Keay, C., Farewell, T., Lilja, H., Juilleret, J., Marx, S., Takata,
770 Y., Kazuyuki, Y., Mansuy, N., Panagos, P., Van Liedekerke, M., Skalsky, R., Sobocka,
771 J., Kobza, J., Eftekhari, K., Alavipanah, S. K., Moussadek, R., Badraoui, M., Da
772 Silva, M., Paterson, G., Gonçalves, M. d. C., Theocharopoulos, S., Yemefack, M.,
773 Tedou, S., Vrscaj, B., Grob, U., Kozák, J., Boruvka, L., Dobos, E., Taboada, M.,
774 Moretti, L., and Rodriguez, D.: Soil legacy data rescue via GlobalSoilMap and other
775 international and national initiatives, *GeoResJ*, 14, 1-19,
776 <https://doi.org/10.1016/j.grj.2017.06.001>, 2017.

777 Arrouays, D., Savin, I., Leenaars, J. , McBratney, A.: *GlobalSoilMap - Digital Soil*
778 *Mapping from Country to Globe*, CRC Press, London, 2018.

779 Ballabio, C., Panagos, P., and Monatanarella, L.: Mapping topsoil physical properties
780 at European scale using the LUCAS database, *Geoderma*, 261, 110-123, 2016.

781 Batjes, N. H.: A taxotransfer rule-based approach for filling gaps in measured soil data
782 in primary SOTER databases, International Soil Reference and Information Centre,
783 Wageningen, 2003.

784 Batjes, N. H.: ISRIC-WISE derived soil properties on a 5 by 5 arc-minutes global
785 grid. Report 2006/02, ISRIC- World Soil Information, Wageningen (with data set),
786 2006.

787 Batjes, N. H.: ISRIC-WISE harmonized global soil profile dataset (ver. 3.1). Report
788 2008/02, ISRIC - World Soil Information, Wageningen, 2008.

789 Batjes, N. H.: Harmonized soil property values for broad-scale modelling
790 (WISE30sec) with estimates of global soil carbon stocks, *Geoderma*, 269, 61-68,
791 <https://doi.org/10.1016/j.geoderma.2016.01.034>, 2016.

792 Batjes, N. H., Ribeiro, E., van Oostrum, A., Leenaars, J., Hengl, T., Mendes de Jesus,

- 793 J.: WoSIS: Serving standardised soil profile data for the world, *Earth Syst. Sci. Data*,
794 9, 1-14, 2017.
- 795 Best, M. J., Pryor, M., Clark, D. B., Rooney, G. G., Essery, R. L. H., Ménard, C. B.,
796 Edwards, J. M., Hendry, M. A., Porson, A., Gedney, N., Mercado, L. M., Sitch, S.,
797 Blyth, E., Boucher, O., Cox, P. M., Grimmond, C. S. B., and Harding, R. J.: The Joint
798 UK Land Environment Simulator (JULES), model description– Part 1: Energy and
799 water fluxes, *Geosci. Model Dev.*, 4, 677-699, 10.5194/gmd-4-677-2011, 2011.
- 800 Bishop, T. F. A., McBratney, A. B., and Laslett, G. M.: Modelling soil attribute depth
801 functions with equal-area quadratic smoothing splines, *Geoderma*, 91, 27–45, 1999.
- 802 Blyth, E. M. a. C.: JULES: A new community land surface mode. *Global Change*
803 *Newsletter*, NO. 66, IGBP, Stockholm, Sweden, 9-11, 2006.
- 804 Brunke, M. A., Tucson, A., Broxton, P. D., Pelletier, J., Gochis, D. J., Hazenberg, P.,
805 Lawrence, D. M., Niu, G. Y., Troch, P. A., and Zeng, X.: Implementation and testing
806 of variable soil depth in the global land surface model CLM4.5, 27th Conference on
807 Climate Variability and Change, Phoenix, 2015,
- 808 Brunke, M. A., Broxton, P., Pelletier, J., Gochis, D., Hazenberg, P., Lawrence, D. M.,
809 Leung, L. R., Niu, G.-Y., Troch, P. A., and Zeng, X.: Implementing and evaluating
810 variable soil thickness in the Community Land Model version 4.5 (CLM4.5), *Journal*
811 *of Climate*, 29, 3441–3461, doi:10.1175/JCLI-D-15-0307.1, 2016.
- 812 Chen, F., and Dudhia, J.: Coupling an advanced land surface-hydrology model with
813 the Penn State-NCAR MM5 modeling system. Part I: Model implementation and
814 sensitivity, *Monthly Weather Review*, 129, 569-585, 2001.
- 815 Chen, Y., Yang, K., Tang, W., Qin, J., and Zhao, L.: Parameterizing soil organic
816 carbon’s impacts on soil porosity and thermal parameters for Eastern Tibet grasslands,
817 *Science China Earth Sciences*, 55, 1001-1011, 10.1007/s11430-012-4433-0, 2012.
- 818 Clapp, R. W., and Hornberger, G. M.: Empirical equations for some soil hydraulic
819 properties, *Water Resources Res.*, 14, 601-604, 1978.
- 820 Clark, D. B., Mercado, L. M., Sitch, S., Jones, C. D., Gedney, N., Best, M. J., Pryor,
821 M., Rooney, G. G., Essery, R. L. H., Blyth, E., Boucher, O., Harding, R. J.,
822 Huntingford, C., and Cox, P. M.: The Joint UK Land Environment Simulator
823 (JULES), model description – Part 2: Carbon fluxes and vegetation dynamics, *Geosci.*
824 *Model Dev.*, 4, 701-722, 10.5194/gmd-4-701-2011, 2011.
- 825 Cooper, M., Mendes, L. M. S., Silva, W. L. C., and Sparovek, G.: A national soil
826 profile database for brazil available to international scientists, *Soil Science Society of*
827 *America Journal*, 69, 649–652, 2005.
- 828 Cox, P. M., Betts, R. A., Bunton, C. B., Essery, R. L. H., Rowntree, P. R., and Smith,

- 829 J.: The impact of new land surface physics on the GCM sensitivity of climate and
830 climate sensitivity, *Climate Dynamics*, 15, 183-203, 1999.
- 831 Dai, Y., Zeng, X., Dickinson, R. E., Baker, I., Bonan, G. B., Bosilovich, M. G.,
832 Denning, A. S., Dirmeyer, P. A., Houser, P. R., Niu, G., Oleson, K. W., Schlosser, C.
833 A., and Yang, Z.: The Common Land Model, *Bull. Amer. Meteor. Soc.*, 84, 1013-
834 1023, 2003.
- 835 Dai, Y., Shangguan, W., Duan, Q., Liu, B., Fu, S., and Niu, G.: Development of a
836 China Dataset of Soil Hydraulic Parameters Using Pedotransfer Functions for Land
837 Surface Modeling, *Journal of Hydrometeorology*, 14, 869–887, 2013.
- 838 De Lannoy, G. J. M., Koster, R. D., Reichle, R. H., Mahanama, S. P. P., and Liu, Q.:
839 An updated treatment of soil texture and associated hydraulic properties in a global
840 land modeling system, *Journal of Advances in Modeling Earth Systems*, 6, 957-979,
841 10.1002/2014ms000330, 2014.
- 842 Dickinson, R. E., Henderson-Sellers, A., and Kennedy, P. J.: Biosphere-Atmosphere
843 Transfer Scheme (BATS) Version 1e as Coupled to the NCAR Community Climate
844 Model. NCAR-TN-387+STR, National Center for Atmospheric Research, Boulder,
845 Colorado, 88, 1993.
- 846 Doney, S. C., Lindsay, K., Fung, I., and John, J.: Natural variability in a stable, 1000-
847 yr global coupled climate-carbon cycle simulation, *Journal of Climate*, 19, 3033-3054,
848 2006.
- 849 Dy, C. Y., and Fung, J. C. H. C. J.: Updated global soil map for the Weather Research
850 and Forecasting model and soil moisture initialization for the Noah land surface
851 model, *Journal of Geophysical Research: Atmospheres*, 121, 8777-8800,
852 10.1002/2015jd024558, 2016.
- 853 Elguindi, N., Bi, X., Giorgi, F., Nagarajan, B., Pal, J., Solmon, F., Rauscher, S., Zakey,
854 A., O'Brien, T., Nogherotto, R., and Giuliani, G.: Regional climatic model RegCM
855 Reference Manual version 4.6, ITCP, Trieste, 33, 2014.
- 856 England, J. R., and Viscarra Rossel, R. A.: Proximal sensing for soil carbon
857 accounting, *SOIL*, 4, 101-122, 10.5194/soil-4-101-2018, 2018.
- 858 Fan, Y., Li, H., and Miguez-Macho, G.: Global Patterns of Groundwater Table Depth,
859 *Science*, 339, 940-943, 10.1126/science.1229881, 2013.
- 860 Guevara, M., Olmedo, G. F., Stell, E., Yigini, Y., Aguilar Duarte, Y., Arellano
861 Hernández, C., Arévalo, G. E., Arroyo-Cruz, C. E., Bolivar, A., Bunning, S.,
862 Bustamante Cañas, N., Cruz-Gaistardo, C. O., Davila, F., Dell Acqua, M., Encina, A.,
863 Figueredo Tacona, H., Fontes, F., Hernández Herrera, J. A., Ibelles Navarro, A. R.,
864 Loayza, V., Manueles, A. M., Mendoza Jara, F., Olivera, C., Osorio Hermosilla, R.,

865 Pereira, G., Prieto, P., Ramos, I. A., Rey Brina, J. C., Rivera, R., Rodríguez-
866 Rodríguez, J., Roopnarine, R., Rosales Ibarra, A., Rosales Riveiro, K. A., Schulz, G.
867 A., Spence, A., Vasques, G. M., Vargas, R. R., and Vargas, R.: No silver bullet for
868 digital soil mapping: country-specific soil organic carbon estimates across Latin
869 America, *SOIL*, 4, 173-193, 10.5194/soil-4-173-2018, 2018.

870 FAO: Soil Map of the World, UNESCO, Paris. Vol. 110, 1971-1981.

871 FAO: Digitized Soil Map of the World and Derived Soil Properties, FAO, Rome,
872 1995.

873 FAO: Digital soil map of the world and derived soil properties, FAO, Land and Water
874 Digital Media Series, CD-ROM, 2003a.

875 FAO: The Digitized Soil Map of the World Including Derived Soil Properties (version
876 3.6), FAO, Rome, 2003b.

877 FAO/IIASA/ISRIC/ISS-CAS/JRC: Harmonized World Soil Database (version1.2),
878 FAO, Rome, Italy and IIASA, Laxenburg, Austria, 2012.

879 Farouki, O. T.: Thermal Properties of Soils. Monograph, No. 81-1, U.S. Army Cold
880 Regions Research and Engineering Laboratory, 1981.

881 Folberth, C., Skalský, R., Moltchanova, E., Balkovič, J., Azevedo, L. B., Obersteiner,
882 M., and van der Velde, M.: Uncertainty in soil data can outweigh climate impact
883 signals in global crop yield simulations, *Nature Communications*, 7, 11872,
884 10.1038/ncomms11872, 2016.

885 Gessler, P.E., Moore, I.D., McKenzie, N.J. and Ryan, P.J.; Soil-landscape modelling
886 and spatial prediction of soil attributes. *International journal of geographical*
887 *information systems*, 9, 421-432, 1995.

888 Global Soil DataTask: Global Soil Data Products CD-ROM (IGBP-DIS). International
889 Geosphere-Biosphere Programme - Data and Information Services, Available online
890 at from the ORNL Distributed Active Archive Center, Oak Ridge National Laboratory,
891 Oak Ridge, Tennessee, U.S.A., 2000.

892 Gong, W., Duan, Q., Li, J., Wang, C., Di, Z., Dai, Y., Ye, A., and Miao, C.: Multi-
893 objective parameter optimization of common land model using adaptive surrogate
894 modeling, *Hydrol. Earth Syst. Sci.*, 19, 2409-2425, doi: 10.5194/hess-19-2409-2015,
895 2015.

896 Gurney, K. R., Baker, D., Rayner, P., and Denning, S.: Interannual variations in
897 continental-scale net carbon exchange and sensitivity to observing networks estimated
898 from atmospheric CO₂ inversions for the period 1980 to 2005, *Global*
899 *Biogeochemical Cycles*, 22, doi:10.1029/2007GB003082, 2008.

900 Hagemann, S., Botzet, M., Dümenil, L., and Machehauer, B.: Derivation of global
901 GCM boundary conditions from 1 km land use satellite data. MPI Report No. 289, 34,
902 1999.

903 Hagemann, S.: An Improved Land Surface Parameter Dataset for Global and Regional
904 Climate Models. MPI Report No. 336, 28, 2002.

905 Hannam, J. A., Hollis, J. M., Jones, R. J. A., Bellamy, P. H., Hayes, S. E., Holden, A.,
906 Van Liedekerke, M. H., and Montanarella, L.: SPADE-2: The soil profile analytical
907 database for Europe, Version 2.0 Beta Version March 2009, unpublished Report,
908 27pp, 2009.

909 Hengl, T., de Jesus, J. M., MacMillan, R. A., Batjes, N. H., Heuvelink, G. B. M.,
910 Ribeiro, E., Samuel-Rosa, A., Kempen, B., Leenaars, J. G. B., Walsh, M. G., and
911 Gonzalez, M. R.: SoilGrids1km — Global Soil Information Based on Automated
912 Mapping, PLoS ONE, 9, e105992, 10.1371/journal.pone.0105992, 2014.

913 Hengl, T., Heuvelink, G. B. M., Kempen, B., Leenaars, J. G. B., Walsh, M. G.,
914 Shepherd, K. D., Sila, A., MacMillan, R. A., Jesus, J. M. d., Tamene, L., and Tondoh,
915 J. E.: Mapping Soil Properties of Africa at 250 m Resolution: Random Forests
916 Significantly Improve Current Predictions, PLOS ONE, 10, e0125814, 2015.

917 Hengl, T., J., M. d. J., Heuvelink, G. B. M., Gonzalez, R., M., K., M. , Blagotic, A.,
918 Shangguan, W., Wright, M. N., Geng, X., Bauer-Marschallinger, B., Guevara, M. A.,
919 Vargas, R., MacMillan, R. A., Batjes, N. H., Leenaars, J. G. B., Ribeiro, E., Wheeler,
920 I., Mantel, S., and Kempen, B.: SoilGrids250m: global gridded soil information based
921 on Machine Learning, PLOS One, 12, 2017.

922 Hiederer, R., and Köchy, M.: Global Soil Organic Carbon Estimates and the
923 Harmonized World Soil Database, Publications Office of the European Union,
924 Luxembourg, 79, 2012.

925 Hoffmann, H., G. Zhao, S. Asseng, M. Bindi, and Christian Biernath, J. C., Elsa
926 Coucheney, Rene Dechow, Luca Doro, Henrik Eckersten, Thomas Gaiser, Balázs
927 Grosz, Florian Heinlein, Belay T. Kassie, Kurt-Christian Kersebaum, Christian Klein,
928 Matthias Kuhnert, Elisabet Lewan, Marco Moriondo, Claas Nendel, Eckart Priesack,
929 Helene Raynal, Pier P. Roggero, Reimund P. Rötter, Stefan Siebert, Xenia Specka,
930 Fulu Tao, Edmar Teixeira, Giacomo Trombi, Daniel Wallach, Lutz Weihermüller,
931 Jagadeesh Yeluripati, Frank Ewert: Impact of Spatial Soil and Climate Input Data
932 Aggregation on Regional Yield Simulations, Plos One, 11, e0151782, 2016.

933 Hugelius, G., Tarnocai, C., Broll, G., Canadell, J. G., Kuhry, P., and Swanson, D. K.:
934 The Northern Circumpolar Soil Carbon Database: spatially distributed datasets of soil
935 coverage and soil carbon storage in the northern permafrost regions, Earth Syst. Sci.
936 Data, 5, 3-13, 10.5194/essd-5-3-2013, 2013.

- 937 Ji, P., Yuan, X., and Liang, X.-Z.: Do Lateral Flows Matter for the Hyperresolution
938 Land Surface Modeling?, *Journal of Geophysical Research: Atmospheres*, 122,
939 12,077-012,092, doi:10.1002/2017JD027366, 2017.
- 940 Johnston, R. M., Barry, S. J., Bleys, E., Bui, E. N., Moran, C. J., Simon, D. A. P.,
941 Carlile, P., McKenzie, N. J., Henderson, B. L., Chapman, G., Imhoff, M., Maschmedt,
942 D., Howe, D., Grose, C., and Schoknecht, N.: ASRIS: the database, *Australian Journal
943 of Soil Research*, 416, 1021-1036, 2003.
- 944 Instituto Nacional de Estadística y Geografía: Conjunto de Datos de Perfiles de Suelos
945 Escala 1: 250 000 Serie II (Continuo Nacional), INEGI, Aguascalientes, Ags. Mexico,
946 2016.
- 947 Jordan, H., Tom, G., Jens, H., and Janine, B.: Compiling and Mapping Global
948 Permeability of the Unconsolidated and Consolidated Earth: GLobal HYdrogeology
949 MaPS 2.0 (GLHYMPS 2.0), *Geophysical Research Letters*, 45, 1897-1904,
950 doi:10.1002/2017GL075860, 2018.
- 951 Karssies, L.: CSIRO National Soil Archive and the National Soil Database (NatSoil).
952 No. v1 in Data Collection, CSIRO, Canberra, 2011.
- 953 Kearney, M. R., and Maino, J. L.: Can next-generation soil data products improve soil
954 moisture modelling at the continental scale? An assessment using a new microclimate
955 package for the R programming environment, *Journal of Hydrology*, 561, 662-673,
956 <https://doi.org/10.1016/j.jhydrol.2018.04.040>, 2018.
- 957 Koster, R. D., and Suarez, M. J.: Modeling the land surface boundary in climate
958 models as a composite of independent vegetation stands, *Journal of Geophysical
959 Research: Atmospheres*, 97, 2697-2715, doi:10.1029/91JD01696, 1992.
- 960 Kowalczyk, E., Stevens, L., Law, R., Dix, M., Wang, Y., Harman, I., Haynes, K.,
961 Sribinovsky, J., Pak, B. and Ziehn, T: The land surface model component of ACCESS:
962 description and impact on the simulated surface climatology, *Australian
963 Meteorological and Oceanographic Journal*, 63, 65–82, 2013.
- 964 Krinner, G., N. Viovy, N. de Noblet-Ducoudré, J. Ogée, J. Polcher, P. Friedlingstein,
965 P. Ciais, S. Sitch, and I. C. Prentice: A dynamic global vegetation model for studies of
966 the coupled atmosphere-biosphere system, *Global Biogeochemical Cycles*, 19,
967 GB1015, 2005.
- 968 Kuhnert, M., Yeluripati, J., Smith, P., Hoffmann, H., van Oijen, M., Constantin, J.,
969 Coucheney, E., Dechow, R., Eckersten, H., Gaiser, T., Grosz, B., Haas, E.,
970 Kersebaum, K.-C., Kiese, R., Klatt, S., Lewan, E., Nendel, C., Raynal, H., Sosa, C.,
971 Specka, X., Teixeira, E., Wang, E., Weihermüller, L., Zhao, G., Zhao, Z., Ogle, S., and
972 Ewert, F.: Impact analysis of climate data aggregation at different spatial scales on
973 simulated net primary productivity for croplands, *European Journal of Agronomy*, 88,

- 974 41-52, <https://doi.org/10.1016/j.eja.2016.06.005>, 2017.
- 975 Landon, J.R., 1991. Booker Tropical Soil Manual. Longman Scientific & Technical,
976 New York.
- 977 Lawrence, P. J., and Chase, T. N.: Representing a new MODIS consistent land surface
978 in the Community Land Model (CLM 3.0), *Journal of Geophysical Research*, 112,
979 10.1029/2006JG000168, 2007.
- 980 Leenaars, J. G. B.: Africa Soil Profiles Database, Version 1.0. A compilation of geo-
981 referenced and standardized legacy soil profile data for Sub Saharan Africa (with
982 dataset). ISRIC report 2012/03, Africa Soil Information Service (AfSIS) project and
983 ISRIC - World Soil Information, Wageningen, the Netherlands, 2012.
- 984 Lei, H., Yang, D., and Huang, M.: Impacts of climate change and vegetation dynamics
985 on runoff in the mountainous region of the Haihe River basin in the past five decades,
986 *Journal of Hydrology*, 511, 786-799, <http://dx.doi.org/10.1016/j.jhydrol.2014.02.029>,
987 2014.
- 988 Li, C., Lu, H., Yang, K., Wright, J. S., Yu, L., Chen, Y., Huang, X., and Xu, S.:
989 Evaluation of the Common Land Model (CoLM) from the Perspective of Water and
990 Energy Budget Simulation: Towards Inclusion in CMIP6, *Atmosphere*, 8, 141, 2017.
- 991 Li, J., Duan, Q., Wang, Y.-P., Gong, W., Gan, Y., and Wang, C.: Parameter
992 optimization for carbon and water fluxes in two global land surface models based on
993 surrogate modelling, *International Journal of Climatology*, 38, e1016-e1031,
994 doi:10.1002/joc.5428, 2018.
- 995 Liang, X., Lettenmaier, D. P., Wood, E. F., and Burges, S. J.: A simple hydrologically
996 based model of land surface water and energy fluxes for general circulation models,
997 *Journal of Geophysical Research: Atmospheres*, 99, 14415-14428,
998 doi:10.1029/94JD00483, 1994.
- 999 Livneh, B., Kumar, R., and Samaniego, L.: Influence of soil textural properties on
1000 hydrologic fluxes in the Mississippi river basin, *Hydrological Processes*, 29, 4638-
1001 4655, [dx.doi.org/10.1002/hyp.10601](https://doi.org/10.1002/hyp.10601), 2015.
- 1002 Looy, K. V., Bouma, J., Herbst, M., Koestel, J., Minasny, B., Mishra, U., Montzka, C.,
1003 Nemes, A., Pachepsky, Y. A., Padarian, J., Schaap, M. G., Tóth, B., Verhoef, A.,
1004 Vanderborght, J., Ploeg, M. J., Weihermüller, L., Zacharias, S., Zhang, Y., and
1005 Vereecken, H.: Pedotransfer Functions in Earth System Science: Challenges and
1006 Perspectives, *Reviews of Geophysics*, 55, 1199-1256, doi:10.1002/2017RG000581,
1007 2017.
- 1008 Luo, Y., Ahlström, A., Allison, S. D., Batjes, N. H., Brovkin, V., Carvalhais, N.,
1009 Chappell, A., Ciais, P., Davidson, E. A., Finzi, A., Georgiou, K., Guenet, B., Hararuk,

1010 O., Harden, J. W., He, Y., Hopkins, F., Jiang, L., Koven, C., Jackson, R. B., Jones, C.
1011 D., Lara, M. J., Liang, J., McGuire, A. D., Parton, W., Peng, C., Randerson, J. T.,
1012 Salazar, A., Sierra, C. A., Smith, M. J., Tian, H., Todd-Brown, K. E. O., Torn, M., van
1013 Groenigen, K. J., Wang, Y. P., West, T. O., Wei, Y., Wieder, W. R., Xia, J., Xu, X., Xu,
1014 X., and Zhou, T. C. G. B.: Toward more realistic projections of soil carbon dynamics
1015 by Earth system models, *Global Biogeochemical Cycles*, 30, 40-56, doi:
1016 10.1002/2015gb005239, 2016.

1017 MacDonald, K. B., and Valentine, K. W. G.: CanSIS/NSDB. A general description
1018 (Centre for Land and Biological Resources Research), Research Branch, Agriculture
1019 Canada, Ottawa, 1992.

1020 Mauritsen, Thorsten, Jürgen Bader, Tobias Becker, Jörg Behrens, Matthias Bittner,
1021 Renate Brokopf, Victor Brovkin, Martin Claussen, Traute Crueger, Monika Esch,
1022 Irina Fast, Stephanie Fiedler, Dagmar Fläschner, Veronika Gayler, Marco Giorgetta,
1023 Daniel S. Goll, Helmuth Haak, Stefan Hagemann, Christopher Hedemann, Cathy
1024 Hohenegger, Tatiana Ilyina, Thomas Jahns, Diego Jimenez de la Cuesta Otero, Johann
1025 Jungclaus, Thomas Kleinen, Silvia Kloster, Daniela Kracher, Stefan Kinne, Deike
1026 Kleberg, Gitta Lasslop, Luis Kornblueh, Jochem Marotzke, Daniela Matei, Katharina
1027 Meraner, Uwe Mikolajewicz, Kameswarrao Modali, Benjamin Möbis, Wolfgang A.
1028 Müller, Julia E. M. S. Nabel, Christine C. W. Nam, Dirk Notz, Sarah-Sylvia Nyawira,
1029 Hanna Paulsen, Karsten Peters, Robert Pincus, Holger Pohlmann, Julia Pongratz, Max
1030 Popp, Thomas Raddatz, Sebastian Rast, Rene Redler, Christian H. Reick, Tim
1031 Rohrschneider, Vera Schemann, Hauke Schmidt, Reiner Schnur, Uwe Schulzweida,
1032 Katharina D. Six, Lukas Stein, Irene Stemmler, Bjorn Stevens, Jin-Song von Storch,
1033 Fangxing Tian, Aiko Voigt, Philipp de Vrese, Karl-Hermann Wieners, Stiig
1034 Wilkenskjeld, Alexander Winkler, and Erich Roeckner: Developments in the MPI-M
1035 Earth System Model version 1.2 (MPI-ESM 1.2) and its response to increasing CO₂,
1036 *Journal of Advances in Modeling Earth Systems*, 2019.

1037 McBratney, A. B., Santos, M. L. M., and Minasny, B.: On digital soil mapping,
1038 *Geoderma*, 117, 3-52, doi: 10.1016/s0016-7061(03)00223-4, 2003.

1039 McBratney, A. B., Minasny, B., and Tranter, G.: Necessary meta-data for pedotransfer
1040 functions, *Geoderma*, 160, 627-629, 2011.

1041 McGuire, A. D., Melillo, J. M., Kicklighter, D. W., Pan, Y. D., Xiao, X. M., Helfrich,
1042 J., Moore, B., Vorosmarty, C. J., and Schloss, A. L.: Equilibrium responses of global
1043 net primary production and carbon storage to doubled atmospheric carbon dioxide:
1044 sensitivity to changes in vegetation nitrogen concentration, *Global Biogeochem.*
1045 *Cycles*, 11, 173-189, 1997.

1046 McLellan, I., Varela, A., Blahgen, M., Fumi, M. D., Hassen, A., Hechminet, N.,
1047 Jaouani, A., Khessairi, A., Lyamlouli, K., Ouzari, H.-I., Mazzoleni, V., Novelli, E.,
1048 Pintus, A., Rodrigues, C., Ruiu, P. A., Pereira, C. S., and Hursthouse, A.:
1049 Harmonisation of physical and chemical methods for soil management in Cork Oak

- 1050 forests - Lessons from collaborative investigations, *African Journal of Environmental*
1051 *Science and Technology*, 7, 386-401, 2013.
- 1052 Melton, J. R., Sospedra-Alfonso, R., and McCusker, K. E.: Tiling soil textures for
1053 terrestrial ecosystem modelling via clustering analysis: a case study with CLASS-
1054 CTEM (version 2.1), *Geosci. Model Dev.*, doi: 10.2761-2783, 10.5194/gmd-10-2761-
1055 2017, 2017.
- 1056 Miller, D. A., and White, R. A.: A conterminous United States multilayer soil
1057 characteristics dataset for regional climate and hydrology modeling, *Earth*
1058 *Interactions*, 2, 1-26, doi: 10.1175/1087-3562(1998)002<0001:ACUSMS>2.3.CO;2,
1059 1998.
- 1060 Minasny, B., McBratney, A.B. and Salvador-Blanes, S.: Quantitative models for
1061 pedogenesis—A review. *Geoderma*, 144, 140-157, 2008.
- 1062 Moigne, P.: SURFEX scientific documentation, Centre National de Recherches
1063 Meteorologiques, 2018
- 1064 Montzka, C., Herbst, M., Weihermüller, L., Verhoef, A., and Vereecken, H.: A global
1065 data set of soil hydraulic properties and sub-grid variability of soil water retention and
1066 hydraulic conductivity curves, *Earth Syst. Sci. Data*, 9, 529-543, doi: 10.5194/essd-9-
1067 529-2017, 2017.
- 1068 Mulder, V. L., Lacoste, M., Richer-de-Forges, A. C., and Arrouays, D.:
1069 GlobalSoilMap France: High-resolution spatial modelling the soils of France up to
1070 two meter depth, *Science of The Total Environment*, 573, 1352-1369,
1071 <http://dx.doi.org/10.1016/j.scitotenv.2016.07.066>, 2016.
- 1072 NationalSoilSurveyOffice: Soil Map of China (in Chinese), China Map Press, Beijing,
1073 1995.
- 1074 Niu, G.-Y., Yang, Z.-L., Mitchell, K. E., Chen, F., Ek, M. B., Barlage, M., Kumar, A.,
1075 Manning, K., Niyogi, D., Rosero, E., Tewari, M., and Xia, Y.: The community Noah
1076 land surface model with multiparameterization options (Noah-MP): 1. Model
1077 description and evaluation with local-scale measurements, *Journal of Geophysical*
1078 *Research: Atmospheres*, 116, doi:10.1029/2010JD015139, 2011.
- 1079 Odgers, N. P., Libohova, Z., and Thompson, J. A.: Equal-area spline functions applied
1080 to a legacy soil database to create weighted-means maps of soil organic carbon at a
1081 continental scale, *Geoderma*, 189-190, 153-163, 2012.
- 1082 Oleson, K. W., D.M. Lawrence, G.B. Bonan, B. Drewniak, M. Huang, C.D. Koven, S.
1083 Levis, F. Li, W.J. Riley, Z.M. Subin, S.C. Swenson, P.E. Thornton, A. Bozbiyik, R.
1084 Fisher, E. Kluzek, J.-F. Lamarque, P.J. Lawrence, L.R. Leung, W. Lipscomb, S.
1085 Muszala, D.M. Ricciuto, W. Sacks, Y. Sun, J. Tang, Z.-L. Yang: Technical Description

1086 of version 4.5 of the Community Land Model (CLM). Ncar Technical Note
1087 NCAR/TN-503+STR, National Center for Atmospheric Research, Boulder, CO, 422,
1088 2013.

1089 Orth, R., Dutra, E. and Pappenberger, F.: Improving Weather Predictability by
1090 Including Land Surface Model Parameter Uncertainty. *Monthly Weather Review*
1091 144(4), 1551-1569, 2016.

1092 Oz, B., V. Deutsch, C., and Frykman, P.: A visualbasic program for histogram and
1093 variogram scaling, *Computers & Geosciences*, 28, 21-31,
1094 [http://dx.doi.org/10.1016/S0098-3004\(01\)00011-5](http://dx.doi.org/10.1016/S0098-3004(01)00011-5), 2002.

1095 Park, J., Kim, H.-S., Lee, S.-J., and Ha, T.: Numerical Evaluation of JULES Surface
1096 Tiling Scheme with High-Resolution Atmospheric Forcing and Land Cover Data,
1097 *SOLA*, 14, 19-24, 10.2151/sola.2018-004, 2018.

1098 Patterson, K. A.: Global distributions of total and total-avaiable soil water-holding
1099 capacities, Master, University of Delawar, Newark, DE, 1990.

1100 Pelletier, J. D., P. D. Broxton, P. Hazenberg, X. Zeng, P. A. Troch, G.-Y. Niu, Z.
1101 Williams, M. A. Brunke, and D. Gochis: A gridded global data set of soil, immobile
1102 regolith, and sedimentary deposit thicknesses for regional and global land surface
1103 modeling, *Journal of Advances in Modeling Earth Systems*, 8, doi:
1104 10.1002/2015MS000526, 2016.

1105 Pillar 5 Working Group: Implementation Plan for Pillar Five of the Global Soil
1106 Partnership, FAO, Rome, 2017.

1107 Pillar four Working Group: Plan of Action for Pillar Four of the Global Soil
1108 Partnership, FAO, Rome, 2014.

1109 Post, D. F., Fimbres, A., Matthias, A. D., Sano, E. E., Accioly, L., Batchily, A. K., and
1110 Ferreira, L. G.: Predicting Soil Albedo from Soil Color and Spectral Reflectance Data,
1111 *Soil Science Society of America Journal* 64, 1027-1034, 2000.

1112 Quattrochi, D. A., Emerson, C. W., Lam, N. S.-N., and Qiu, H.-l.: Fractal
1113 Characterization of Multitemporal Remote Sensing Data, in: *Modelling Scale in*
1114 *Geographical Information System*, edited by: Tate, N., and Atkinson, P., John Wiley &
1115 Sons, Lodon, 13-34, 2001.

1116 Ramcharan, A., Hengl, T., Nauman, T., Brungard, C., Waltman, S., Wills, S., and
1117 Thompson, J.: Soil Property and Class Maps of the Conterminous United States at
1118 100-Meter Spatial Resolution, *Soil Science Society of America Journal*, 82, 186-201,
1119 doi: 10.2136/sssaj2017.04.0122, 2018.

1120 Ribeiro, E., Batjes, N. H., and Oostrum, A. v.: World Soil Information Service
1121 (WoSIS) - Towards the standardization and harmonization of world soil data, ISRIC -

- 1122 World Soil Information, Wageningen, 2018.
- 1123 Reynolds, C. A., Jackson, T. J., and Rawls, W. J.: Estimating soil water-holding
1124 capacities by linking the Food and Agriculture Organization Soil map of the world
1125 with global pedon databases and continuous pedotransfer functions, *Water Resour.*
1126 *Res.*, 36, 3653-3662, 2000.
- 1127 Romanowicz, A. A., Vanclooster, M., Rounsevell, M., and Junesse, I. L.: Sensitivity
1128 of the SWAT model to the soil and land use data parametrisation: a case study in the
1129 Thyle catchment, Belgium, *Ecological Modelling*, 187, 27-39, 2005.
- 1130 Rosenzweig, C., and Abramopoulos, F.: Land surface model development for the
1131 GISS GCM, *J. Climate*, 10, 2040-2054, 1997.
- 1132 Ross, C. W., Prihodko, L., Anchang, J., Kumar, S., Ji, W., and Hanan, N. P.:
1133 HYSOGs250m, global gridded hydrologic soil groups for curve-number-based runoff
1134 modeling, *Scientific Data*, 5, 180091, 10.1038/sdata.2018.91, 2018.
- 1135 Rotstayn, L. D., S. J. Jeffrey, M. A. Collier, S. M. Dravitzki, A. C. Hirst, J. I. Syktus,
1136 and K. K. Wong: Aerosol- and greenhouse gas-induced changes in summer rainfall
1137 and circulation in the Australasian region: a study using single-forcing climate
1138 simulations, *Atmos. Chem. Phys.*, 12, 6377–6404, 2012.
- 1139 Saha, S., Moorthi, S., Wu, X., Wang, J., Nadiga, S., Tripp, P., Behringer, D., Hou, Y.-
1140 T., Chuang, H.-y., Iredell, M., Ek, M., Meng, J., Yang, R., Mendez, M.P., Dool, H.v.d.,
1141 Zhang, Q., Wang, W., Chen, M. and Becker, E.: The NCEP Climate Forecast System
1142 Version 2. *Journal of Climate* 27(6), 2185-2208, 2014.
- 1143 Sanchez, P. A., Ahamed, S., Carré, F., Hartemink, A. E., Hempel, J., Huising, J.,
1144 Lagacherie, P., McBratney, A. B., McKenzie, N. J., Mendonça-Santos, M. d. L.,
1145 Budiman Minasny, L. M., Okoth, P., Palm, C. A., Sachs, J. D., Shepherd, K. D.,
1146 Vågen, T.-G., Vanlauwe, B., Walsh, M. G., Winowiecki, L. A., and Zhang, G.-L.:
1147 Digital soil map of the world, *Science*, 325, 680-681, 2009.
- 1148 Sellers, P. J., Randall, D. A., Collatz, G. J., Berry, J. A., Field, C. B., Dazlich, D. A.,
1149 Zhang, C., Collelo, G. D., and Bounoua, L.: A revised land surface parameterization
1150 (SiB2) for atmospheric GCMs. Part I: model formulation, *Journal of Climate*, 9, 676-
1151 705, 1996.
- 1152 Shangguan, W., Dai, Y., Liu, B., Ye, A., and Yuan, H.: A soil particle-size distribution
1153 dataset for regional land and climate modelling in China, *Geoderma*, 171-172, 85-91,
1154 2012.
- 1155 Shangguan, W., Dai, Y., Liu, B., Zhu, A., Duan, Q., Wu, L., Ji, D., Ye, A., Yuan, H.,
1156 Zhang, Q., Chen, D., Chen, M., Chu, J., Dou, Y., Guo, J., Li, H., Li, J., Liang, L.,
1157 Liang, X., Liu, H., Liu, S., Miao, C., and Zhang, Y.: A China dataset of soil properties

- 1158 for land surface modeling, *Journal of Advances in Modeling Earth Systems*, 5, 212-
1159 224, doi: 10.1002/jame.20026, 2013.
- 1160 Shangguan, W.: Comparison of aggregation ways on soil property maps, 20th World
1161 Congress of Soil Science, Jeju, Korea, 2014,
- 1162 Shangguan, W., Dai, Y., Duan, Q., Liu, B., and Yuan, H.: A global soil data set for
1163 earth system modeling, *Journal of Advances in Modeling Earth Systems*, 6, 249-263,
1164 2014.
- 1165 Shangguan, W., Hengl, T., Mendes de Jesus, J., Yuan, H., and Dai, Y.: Mapping the
1166 global depth to bedrock for land surface modeling, *Journal of Advances in Modeling
1167 Earth Systems*, 9, 65-88, doi: 10.1002/2016ms000686, 2017.
- 1168 Shoba, S. A., Stolbovoi, V. S., Alyabina, I. O., and Molchanov, E. N.: Soil-geographic
1169 database of Russia, *Eurasian Soil Science*, 41, doi: 907-913,
1170 10.1134/s1064229308090019, 2008.
- 1171 Singh, R. S., Reager, J. T., Miller, N. L., and Famiglietti, J. S.: Toward hyper-
1172 resolution land-surface modeling: The effects of fine-scale topography and soil
1173 texture on CLM4.0 simulations over the Southwestern U.S, *Water Resources
1174 Research*, 51, 2648-2667, doi:10.1002/2014WR015686, 2015.
- 1175 Slevin, D., Tett, S. F. B., Exbrayat, J. F., Bloom, A. A., and Williams, M.: Global
1176 evaluation of gross primary productivity in the JULES land surface model v3.4.1,
1177 *Geosci. Model Dev.*, 10, 2651-2670, 10.5194/gmd-10-2651-2017, 2017.
- 1178 Soil Survey Staff, N. R. C. S., United States Department of Agriculture: Web Soil
1179 Survey. Available online at <http://websoilsurvey.nrcs.usda.gov/>. Accessed 1/1/2017,
1180 2017.
- 1181 Soil Landscapes of Canada Working Group: Soil Landscapes of Canada version 3.2.,
1182 Agriculture and Agri-Food Canada, Ottawa, Ontario, 2010.
- 1183 Stoorvogel, J. J., Bakkenes, M., Temme, A. J. A. M., Batjes, N. H., and Brink, B. J.
1184 E.: S-World: A Global Soil Map for Environmental Modelling, *Land Degradation &
1185 Development*, 28, 22-33, doi:10.1002/ldr.2656, 2017.
- 1186 Takata, K., Emori, S., and Watanabe, T.: Development of the minimal advanced
1187 treatments of surface interaction and runoff. *Global Planet. Change*, 38, 209–222,
1188 2003.
- 1189 Thompson, J. A., Prescott, T., Moore, A. C., Bell, J., Kautz, D. R., Hempel, J. W.,
1190 Waltman, S. W., and Perry, C. H.: Regional approach to soil property mapping using
1191 legacy data and spatial disaggregation techniques, 19th World Congress of Soil
1192 Science, Brisbane, Queensland, 2010,

- 1193 Thornton, P. E., and Rosenbloom, N. A.: Ecosystem model spin-up: estimating steady
1194 state conditions in a coupled terrestrial carbon and nitrogen cycle model, *Ecological*
1195 *Modelling*, 189, 25-48, 2005.
- 1196 Tian, W., Li, X., Wang, X. S., and Hu, B. X.: Coupling a groundwater model with a
1197 land surface model to improve water and energy cycle simulation, *Hydrol. Earth Syst.*
1198 *Sci. Discuss.*, 2012, doi: 1163-1205, 10.5194/hessd-9-1163-2012, 2012.
- 1199 Tifafi, M., Guenet, B., and Hatté, C.: Large Differences in Global and Regional Total
1200 Soil Carbon Stock Estimates Based on SoilGrids, HWSD, and NCSCD:
1201 Intercomparison and Evaluation Based on Field Data From USA, England, Wales, and
1202 France, *Global Biogeochemical Cycles*, 32, 42-56, doi:10.1002/2017GB005678,
1203 2018. Todd-Brown, K. E. O., Randerson, J. T., Post, W. M., Hoffman, F. M., Tarnocai,
1204 C., Schuur, E. A. G., and Allison, S. D.: Causes of variation in soil carbon simulations
1205 from CMIP5 Earth system models and comparison with observations,
1206 *Biogeosciences*, 10, 1717-1736, doi: 10.5194/bg-10-1717-2013, 2013.
- 1207 Todd-Brown, K. E. O., Randerson, J. T., Hopkins, F., Arora, V., Hajima, T., Jones, C.,
1208 Shevliakova, E., Tjiputra, J., Volodin, E., Wu, T., Zhang, Q., and Allison, S. D.:
1209 Changes in soil organic carbon storage predicted by Earth system models during the
1210 21st century, *Biogeosciences*, 11, 2341-2356, doi: 10.5194/bg-11-2341-2014, 2014.
- 1211 Tóth, B., Weynants, M., Nemes, A., Makó, A., Bilas, G., and Tóth, G.: New
1212 generation of hydraulic pedotransfer functions for Europe, *European Journal of Soil*
1213 *Science*, 66, 226-238, doi:10.1111/ejss.12192, 2015.
- 1214 Tóth, B., Weynants, M., Pásztor, L., and Hengl, T.: 3D soil hydraulic database of
1215 Europe at 250 m resolution, *Hydrological Processes*, 31, 2662-2666,
1216 doi:10.1002/hyp.11203, 2017.
- 1217 Trinh, T., Kavvas, M. L., Ishida, K., Ercan, A., Chen, Z. Q., Anderson, M. L., Ho, C.,
1218 and Nguyen, T.: Integrating global land-cover and soil datasets to update saturated
1219 hydraulic conductivity parameterization in hydrologic modeling, *Science of The Total*
1220 *Environment*, 631-632, 279-288, <https://doi.org/10.1016/j.scitotenv.2018.02.267>,
1221 2018.
- 1222 Van Engelen, V., and Dijkshoorn, J.: Global and National Soils and Terrain Digital
1223 Databases (SOTER), Procedures Manual, version 2.0. ISRIC Report 2012/04, ISRIC -
1224 World Soil Information, Wageningen, the Netherlands, 2012.
- 1225 Vaysse, K., and Lagacherie, P.: Using quantile regression forest to estimate
1226 uncertainty of digital soil mapping products, *Geoderma*, 291, 55-64,
1227 <https://doi.org/10.1016/j.geoderma.2016.12.017>, 2017.
- 1228 Vereecken, H., Weynants, M., Javaux, M., Pachepsky, Y., Schaap, M. G., and
1229 Genuchten, M. T. v.: Using pedotransfer functions to estimate the van Genuchten-

- 1230 Mualem soil hydraulic properties: a review, *Vadose Zone Journal*, 9, 795-820, 2010.
- 1231 Viscarra Rossel, R., Chen, C., Grundy, M., Searle, R., Clifford, D., and Campbell, P.:
1232 The Australian three-dimensional soil grid: Australia's contribution to the
1233 GlobalSoilMap project, *Soil Research*, 53, 845-864, 2015.
- 1234 Verseghy, D.: The Canadian land surface scheme (CLASS): Its history and future,
1235 *Atmosphere-Ocean*, 38:1, 1-13, 2000.
- 1236 Vrettas, M. D., and Fung, I. Y.: Toward a new parameterization of hydraulic
1237 conductivity in climate models: Simulation of rapid groundwater fluctuations in
1238 Northern California, *Journal of Advances in Modeling Earth Systems*, 7, 2105-2135,
1239 doi: 10.1002/2015ms000516, 2016.
- 1240 Wang, G., Gertner, G., and Anderson, A. B.: Up-scaling methods based on variability-
1241 weighting and simulation for inferring spatial information across scales, *International*
1242 *Journal of Remote Sensing*, 25, 4961- 4979, 2004.
- 1243 Webb, R. S., Rosenzweig, C. E., and Levine, E. R.: Specifying land surface
1244 characteristics in general circulation models: Soil profile data set and derived water-
1245 holding capacities, *Global Biogeo. Cyc.*, 7, 97-108, 1993.
- 1246 Wilson, M. F., and Henderson-Sellers, A.: A global archive of land cover and soils
1247 data for use in general circulation climate models, *Journal of Climatology*, 5, 119-143,
1248 1985.
- 1249 Wu, L., Wang, A., and Sheng, Y.: Impact of Soil Texture on the Simulation of Land
1250 Surface Processes in China, *Climatic and Environmental Research (in Chinese)*, 19,
1251 559-571, doi:10.3878/j.issn.1006-9585.2013.13055, 2014.
- 1252 Wu, T., Song, L., Li, W., Wang, Z., Zhang, H., Xin, X., Zhang, Y., Zhang, L., Li, J.,
1253 Wu, F., Liu, Y., Zhang, F., Shi, X., Chu, M., Zhang, J., Fang, Y., Wang, F., Lu, Y., Liu,
1254 X., Wei, M., Liu, Q., Zhou, W., Dong, M., Zhao, Q., Ji, J., Li, L. and Zhou, M: An
1255 overview of BCC climate system model development and application for climate
1256 change studies. *Journal of Meteorological Research*, 28(1), 34-56, 2014. Wu, X., Lu,
1257 G., Wu, Z., He, H., Zhou, J., and Liu, Z.: An Integration Approach for Mapping Field
1258 Capacity of China Based on Multi-Source Soil Datasets, *Water*, 10, 728, 2018.
- 1259 Zhang, W. L., Xu, A. G., Ji, H. J., Zhang, R. L., Lei, Q. L., Zhang, H. Z., Zhao, L. P.,
1260 and Long, H. Y.: Development of China digital soil map at 1:50,000 scale, 19th World
1261 Congress of Soil Science, *Soil Solutions for a Changing World*, Brisbane, Australia,
1262 2010,
- 1263 Zhao, H., Zeng, Y., Lv, S., and Su, Z.: Analysis of soil hydraulic and thermal
1264 properties for land surface modeling over the Tibetan Plateau, *Earth Syst. Sci. Data*,
1265 10, doi: 1031-1061, 10.5194/essd-10-1031-2018, 2018a.

1266 Zhao, M., Golaz, J.-C., Held, I. M., Guo, H., Balaji, V., Benson, R., Chen, J.-H.,
1267 Chen, X., Donner, L. J., Dunne, J. P., Dunne, K., Durachta, J., Fan, S.-M.,
1268 Freidenreich, S. M., Garner, S. T., Ginoux, P., Harris, L. M., Horowitz, L. W.,
1269 Krasting, J. P., Langenhorst, A. R., Liang, Z., Lin, P., Lin, S.-J., Malyshev, S. L.,
1270 Mason, E., Milly, P. C. D., Ming, Y., Naik, V., Paulot, F., Paynter, D., Phillipps, P.,
1271 Radhakrishnan, A., Ramaswamy, V., Robinson, T., Schwarzkopf, D., Seman, C. J.,
1272 Shevliakova, E., Shen, Z., Shin, H., Silvers, L. G., Wilson, J. R., Winton, M.,
1273 Wittenberg, A. T., Wyman, B., and Xiang, B.: The GFDL Global Atmosphere and
1274 Land Model AM4.0/LM4.0: 2. Model Description, Sensitivity Studies, and Tuning
1275 Strategies, *Journal of Advances in Modeling Earth Systems*, 10, 735-769,
1276 doi:10.1002/2017MS001209, 2018b.

1277 Zheng, G., Yang, H., Lei, H., Yang, D., Wang, T., and Qin, Y.: Development of a
1278 Physically Based Soil Albedo Parameterization for the Tibetan Plateau, *Vadose Zone*
1279 *Journal*, 17, doi: 10.2136/vzj2017.05.0102, 2018.

1280 Zheng, H., and Yang, Z. L.: Effects of soil type datasets on regional terrestrial water
1281 cycle simulations under different climatic regimes, *Journal of Geophysical Research:*
1282 *Atmospheres*, Accepted, doi: 10.1002/2016jd025187, 2016.

1283 Zhou, T., Shi, P. J., Jia, G. S., Dai, Y. J., Zhao, X., Shangguan, W., Du, L., Wu, H., and
1284 Luo, Y. Q.: Age-dependent forest carbon sink: Estimation via inverse modeling,
1285 *Journal of Geophysical Research-Biogeosciences*, 120, 2473-2492, doi:
1286 10.1002/2015jg002943, 2015.

1287 Zöbler, L.: A world soil file for global climate modeling, NASA Tech. Memo. 87802,
1288 NASA, New York, 33, 1986.

1289
1290

Table 1. Lists of the soil dataset used by land surface models (LSM) of Earth System Models (ESM) or climate models (CM).

| Dataset | Resolution | ESM or CM | LSM | Input soil data |
|--|------------------------|-------------------------------------|--|--|
| Elguindi et al. (2014) | | RegCM | BATS1e (Dickinson et al., 1993) or CLM4.5 (Oleson et al., 2013) | Soil texture classes and Soil color classes prescribed for BATS vegetation/land cover type |
| FAO (2003 a, b) | 5' | CanESM2 | CTEM (Arora et al., 2009) CLASS3.4 (Verseghy, 2000) | Soil texture |
| FAO (2003 a, b) | 5' | EC-EARTH | HTESSEL (Orth et al., 2016) | Soil texture classes |
| FAO (2003 a, b; outside Conterminous US) STATSGO (Miller and White, 1998) | 5' 30" | WRF CWRF | Noah (Chen and Dudhia, 2001) Noah-MP (Niu et al., 2011) CLM4 Other LSMs | Soil texture |
| GSDE (Shangguan et al., 2014) | 30" | CAS_ESM BNU_ESM GRAPES | CoLM 2014(Dai et al., 2014) | Soil texture, gravel, soil organic carbon, bulk density |
| GSDE (Shangguan et al., 2014) | 30" | WRF CWRF | Noah (Chen and Dudhia, 2001) Noah-MP (Niu et al., 2011) CLM4.5 Other LSMs | Soil texture |
| GSDE (Shangguan et al., 2014) | 30" | BCC_CSM 1.1 BCC_CSM 1.1(m) | BCC_AVIM 1.1 (Wu et al., 2014) | Soil texture |
| Hagemann (2002) | 0.5° (8km over Africa) | MPI-ESM ICON-ESM | JSBACH4 (Mauritsen et al. (2019) | Soil albedo |

| | | | | |
|---|-----------|---|---|---|
| Hagemann (2002) | 0.5° | MPI-ESM ICON-ESM | JSBACH4 (Mauritsen et al. (2019)) | Field capacity, Plant-available soil water holding capacity and wilting point prescribed for ecosystem type |
| Hagemann et al. (1999) | 0.5° | MPI-ESM ICON-ESM | JSBACH4 (Mauritsen et al. (2019)) | Volumetric heat capacity and thermal diffusivity prescribed for 5 soil types of FAO soil map |
| HWSD (FAO/IIASA/ISRIC/ISS -CAS/JRC, 2012) | 30" | GFDL ESM | GFDL LM4 (Zhao et al., 2018b) | Soil texture classes |
| HWSD (FAO/IIASA/ISRIC/ISS -CAS/JRC, 2012) | 30" | HadCM3 HadGEM2 QUEST | JULES/MOSESvn 5.4 (Best et al., 2011; Clark et al., 2011) | Soil texture |
| HWSD (FAO/IIASA/ISRIC/ISS -CAS/JRC, 2012) | 30" | CNRM- CM5 | SURFEX8.1 (Moigne,2018) | Soil texture, soil organic matter |
| IGBP-DIS (Global Soil Data Task, 2000) | 5' | CESM CCSM CMCC– CESM FIO-ESM FGOALS (s2,gl,g2) NorESM1 | CLM 3.0 or CLM 4.0 or CLM 4.5 | Soil texture (sand, clay) |
| | | CESM CCSM CMCC– CESM FIO-ESM FGOALS (s2,gl,g2) NorESM1 | | |
| ISRIC-WISE (Batjes, 2006) combined with NCSD (Hugelius et al., 2013) | 5', 0.25° | CESM CCSM CMCC– CESM FIO-ESM FGOALS (s2,gl,g2) NorESM1 | CLM 3.0 or CLM 4.0 or CLM 4.5 | Soil organic matter |

| | | | | |
|--------------------------------------|-------|---|---|----------------------|
| Lawrence and Chase (2007) | 0.05° | CESM CCSM CMCC- CESM FIO-ESM FGOALS (s2,gl,g2) NorESM1 | CLM 3.0 or CLM 4.0 or CLM 4.5 | Soil color class |
| | | | Mosaic (Koster and Suarez, 1992) | |
| | | | Noah (Chen and Dudhia, 2001) | Soil texture classes |
| Reynolds et al. (2000) | 5' | GLDAS | VIC (Liang et al., 1994) | |
| Webb et al. (1993) and Zöbler (1986) | 1° | GISS-E2 | GISS-LSM (Rosenzweig and Abramopoulos, 1997) | Soil texture |
| Wilson and Henderson-Sellers (1985) | 1° | HadCM3 HadGEM2 QUEST | JULES/MOSESvn 5.4 (Best et al., 2011; Clark et al., 2011) | Soil texture |
| Zöbler (1986) | 1° | ACCESS- ESM | CABLE2.0 (Kowalczyk et al, 2013) | Soil texture classes |
| Zöbler (1986) | 1° | | SiB (Sellers et al., 1996; Gurney et al., 2008) | Soil texture classes |
| Zöbler (1986) | 1° | CFSv2 | CFSv2/Noah(Saha et al., 2014) | Soil texture |
| Zöbler (1986) | 1° | CSIRO- Mk3.6.0 | CSIRO-Mk3.6.0 (Rotstayn et al., 2012) | Soil texture classes |
| Zöbler (1986) | 1° | MIROC (4h,5) MIROC- ESM | MATSIRO (Takata et al., 2003) | Soil texture classes |

| | Zöbler (1986); Reynolds et al. (2000) | 1°, 5' | IPSL-CM6 | ORCHIDEE [rev 3977] (Krinner, 2005) | Soil texture classes |
|------|---|--------|----------|--|----------------------|
| 1291 | | | | | |
| 1292 | ACCESS = Australia Community Climate and Earth System Simulator | | | | |
| 1293 | BATS = Biosphere-Atmosphere Transfer Scheme | | | | |
| 1294 | BCC_CSM = Beijing Climate Center Climate System Model | | | | |
| 1295 | BCC_AVIM = Beijing Climate Center Atmosphere and Vegetation Interaction Model | | | | |
| 1296 | BNU_ESM = Beijing Normal University Earth System Model | | | | |
| 1297 | CABLE = Community Atmosphere Biosphere Land Exchange | | | | |
| 1298 | CanESM = Canadian Earth System Model | | | | |
| 1299 | CAS_ESM = Chinese Academy of Sciences Earth System Model | | | | |
| 1300 | CCSM = Community Climate System Model. | | | | |
| 1301 | CESM = Community Earth System Model | | | | |
| 1302 | CFS = Climate Forecast System | | | | |
| 1303 | CLASS = Canadian Land Surface Scheme | | | | |
| 1304 | CLM = Community Land Model | | | | |
| 1305 | CMCC-CESM = Euro-Mediterranean Centre on Climate Change Community Earth System Model | | | | |
| 1306 | CNRM-CM = Centre National de Recherches Meteorologiques Climate Model | | | | |
| 1307 | CoLM = Common Land Model | | | | |
| 1308 | CSIRO-Mk = Commonwealth Scientific and Industrial Research Organization climate system model | | | | |
| 1309 | CTEM = Canadian Terrestrial Ecosystem Model | | | | |
| 1310 | EC-EARTH = European community Earth-System Model | | | | |
| 1311 | FAO = Food and Agriculture Organization (FAO-UNESCO) digital Soil Map of the World (SMW) at a 1:5 million scale | | | | |
| 1312 | FGOALS = Flexible Global Ocean-Atmosphere-Land System Model | | | | |
| 1313 | FIO-ESM = First Institute of Oceanography Earth System Model | | | | |
| 1314 | GRAPES = Global/Regional Assimilation Prediction System | | | | |
| 1315 | GFDL = Geophysical Fluid Dynamics Laboratory | | | | |
| 1316 | GISS = Goddard Institute for Space Studies | | | | |
| 1317 | GLDAS = Global Land Data Assimilation System | | | | |
| 1318 | GSDE = Global Soil Dataset for Earth System Model | | | | |
| 1319 | HadCM = Hadley Centre Coupled Model | | | | |

1320 HadGEM2-ES = Hadley Global Environment Model 2 - Earth System
1321 HTESEL = Tiled ECMWF Scheme for Surface Exchanges over Land
1322 HWSO = Harmonized World Soil Database
1323 ICON-ESM = Icosahedral non-hydrostatic Earth System Model
1324 IGBP-IDS = Data and Information System of International Geosphere-Biosphere Program
1325 IPSL-CM = Institute Pierre Simon Laplace Climate Model
1326 ISRIC-WISE = World Inventory of Soil Emission Potentials of International Soil Reference and Information Centre
1327 JSBACH = Jena Scheme of Atmosphere Biosphere Coupling in Hamburg
1328 JULES/MOSES= Joint UK Land Environment Simulator/Met Office Surface Exchange Scheme
1329 MATSIRO = Minimal Advanced Treatments of Surface Interaction and Runoff
1330 MIROC = Model for Interdisciplinary Research on Climate
1331 MPI-ESM = Max Planck Institute for Meteorology Earth System Model
1332 Noah-MP = Noah-multiparameterization
1333 NorESM1 = Norwegian Earth System Model
1334 NCSD = Northern Circumpolar Soil Carbon Database
1335 ORCHIDEE = Organising Carbon and Hydrology In Dynamic Ecosystems
1336 QUEST = Quantifying and Understanding the Earth System
1337 RegCM = Regional Climate Model
1338 SiB = Simple Biosphere Model
1339 STATSGO = State Soil Geographic Database
1340 SURFEX = Surface Externalisée
1341 WRF = Weather Research and Forecasting Model

1342

1343

Table 2 Four new global soil datasets for ESM updates.

| Dataset | Resolution | Number of layers | Number of properties | depth to the bottom of a layer (cm) | Mapping method |
|-----------|------------|------------------|----------------------|--|----------------------|
| HWSD | 1km | 2 | 22 | 30, 100 | Linkage method |
| GSDE | 1km | 8 | 39 | 4.5, 9.1, 16.6, 28.9, 49.3, 82.9, 138.3, 229.6 | Linkage method |
| WISE30sec | 1km | 7 | 20 | 20,40,60,80,100,150,200 | Linkage method |
| SoilGrids | 250m | 6 | 7 | 5, 15, 30, 60, 100, 200 | Digital soil mapping |

1344

Table 3 Derived soil properties considered in four global soil datasets.

| Soil property* | HWSD | GSDE | WISE30sec | SoilGrids | Soil property* | HWSD | GSDE | WISE30sec | SoilGrids |
|----------------------|------|------|-----------|-----------|-----------------------------------|------|------|-----------|-----------|
| Drainage class | √ | √ | √ | | Total carbon | | √ | | |
| AWC class | √ | √ | | | Total nitrogen | | √ | √ | |
| Soil phase | √ | √ | | | Total sulfur | | √ | | |
| Impermeable layer | √ | √ | | | pH(KCL) | | √ | | √ |
| Obstacle to roots | √ | √ | | | pH(CaCl ₂) | | √ | | |
| Additional property | √ | √ | | | Exchangeable Ca | | √ | | |
| Soil water regime | √ | √ | | | Exchangeable Mg | | √ | | |
| Reference soil depth | √ | √ | | | Exchangeable K | | √ | | |
| Depth to bedrock | | | | √ | Exchangeable Na | | √ | | |
| Gravel | √ | √ | √ | √ | Exchangeable Al | | √ | | |
| Sand, Silt, Clay | √ | √ | √ | √ | Exchangeable H | | √ | | |
| Texture class** | √ | | | | VWC at -10 kPa | | √ | | |
| Bulk density | √ | √ | √ | √ | VWC at -33 kPa | | √ | √ | |
| Organic Carbon | √ | √ | √ | √ | VWC at -1500 kPa | | √ | √ | |
| pH(H ₂ O) | √ | √ | √ | √ | Phosphorous by Bray method | | √ | | |
| CEC (clay) | √ | | √ | | Phosphorous by Olsen method | | √ | | |
| CEC (soil) | √ | √ | √ | | Phosphorous by New Zealand method | | √ | | |
| Effective CEC | | | √ | | Water soluble phosphorous | | √ | | |
| Base saturation | √ | √ | √ | | Phosphorous by Mechlich method | | √ | | |

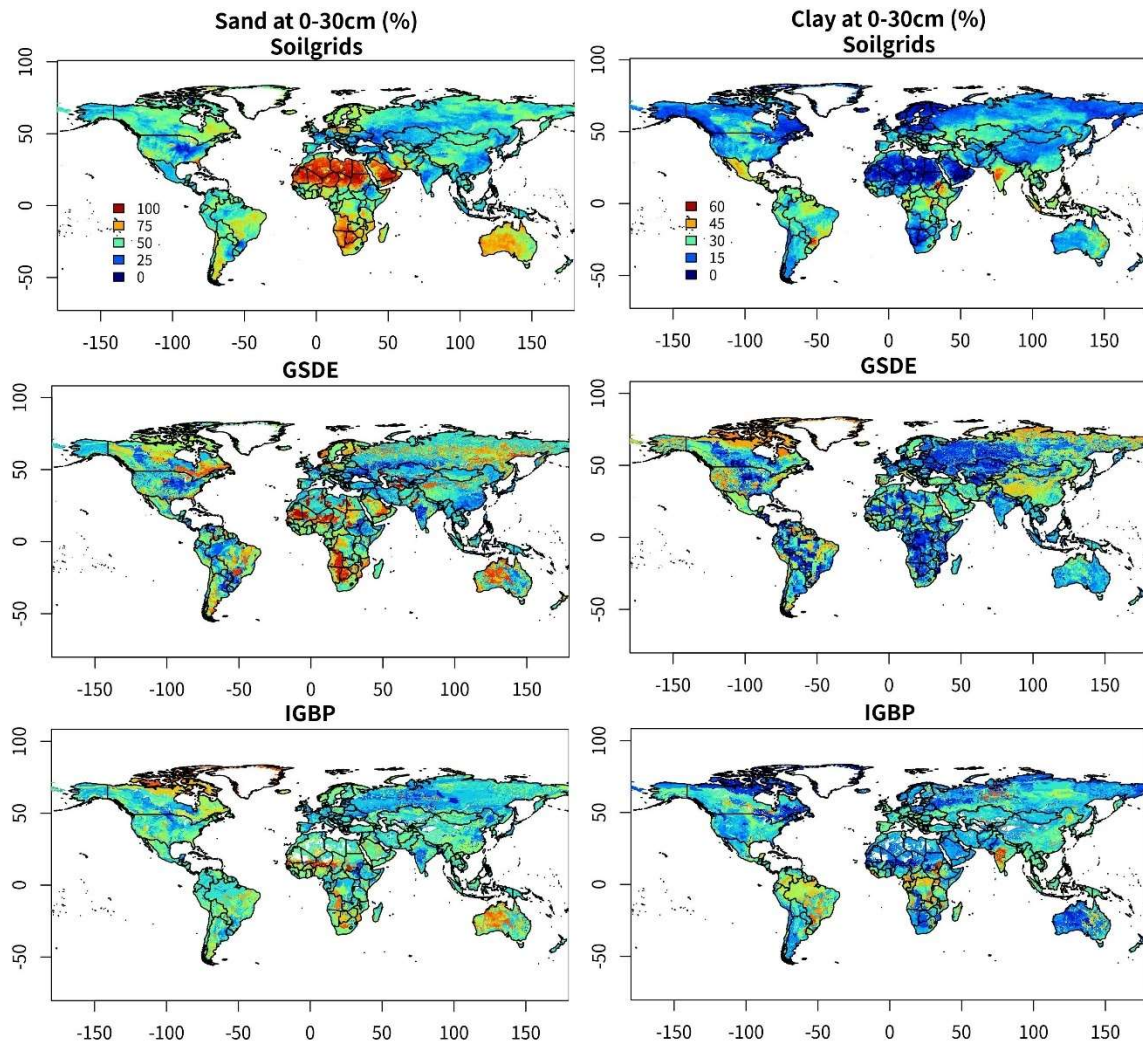
| | | | | | | | |
|-------------------|---|---|---|----------------------|---|---|---|
| TEB | √ | | √ | Total phosphorous | | √ | |
| Calcium Carbonate | √ | √ | √ | Total Potassium | | √ | |
| Gypsum | √ | √ | √ | Salinity (ECE) | √ | √ | √ |
| Sodicity (ESP) | √ | | √ | Aluminium saturation | | | √ |
| C/N ratio | | | √ | | | | |

1346 *CEC is cation exchange capacity. The base saturation measures the sum of exchangeable cations (nutrients) Na, Ca, Mg and K as a
1347 percentage of the overall exchange capacity of the soil (including the same cations plus H and Al). TEB is the total exchangeable base
1348 including Na, Ca, Mg and K. ESP is the exchangeable sodium percentage, which is calculated as $Na * 100 / CEC_{soil}$. ECE is electrical
1349 conductivity. AWC is the available water storage capacity. The first 9 soil properties on the left, including the drainage class and
1350 AWC class are available for each soil type, while the other properties are available for each layer. Notably, many different analytical
1351 methods have been used to derive a given soil property, which is a major source of uncertainty.
1352 **texture class can be calculated using sand, silt and clay content.

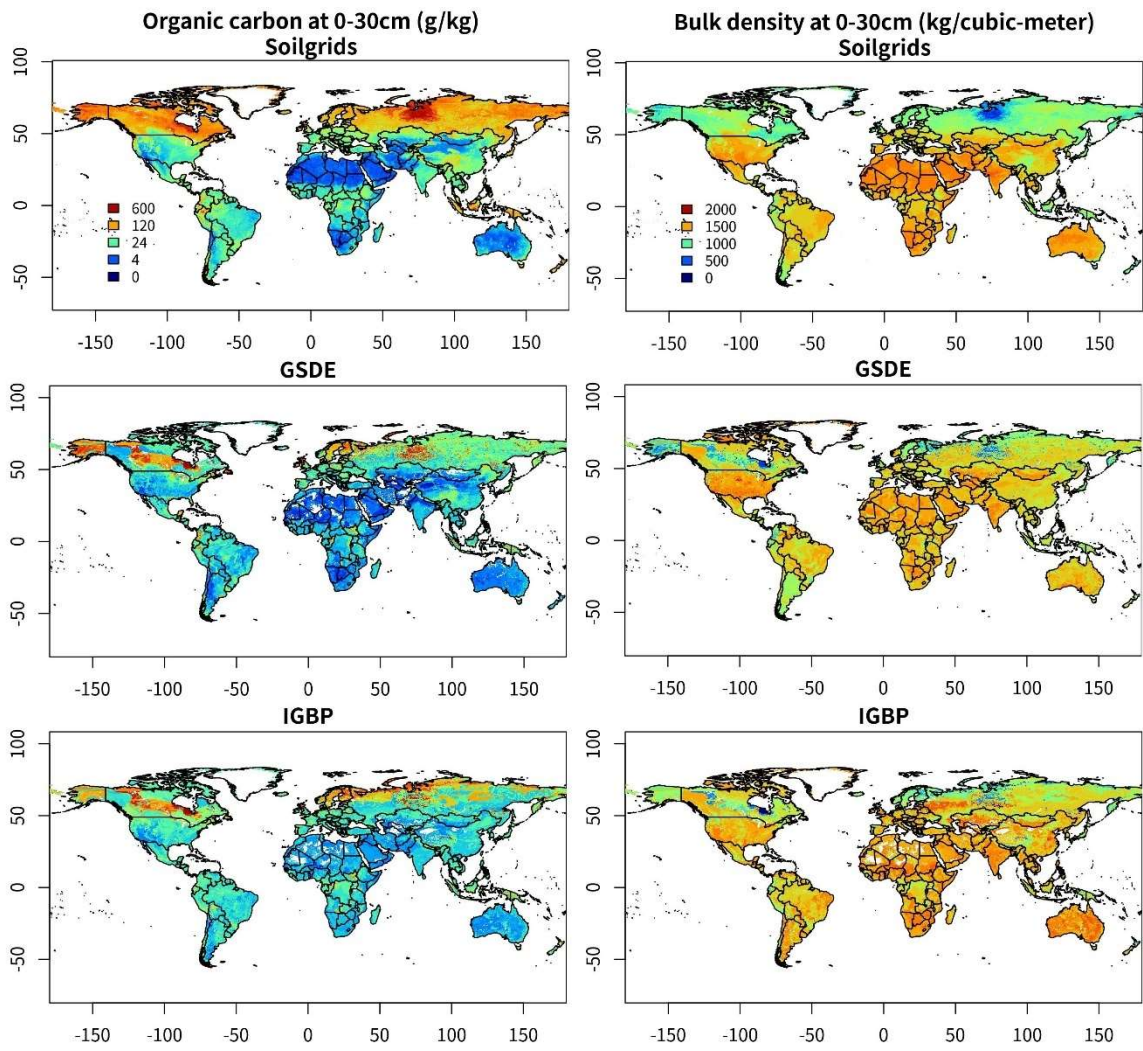
1353 Table 4 Evaluation statistics of soil datasets using soil profiles from World Soil
 1354 Information Service (WoSIS).

| Soil property | Dataset | Topsoil (0-30 cm)* | | | | Subsoil (30-100 cm) | | | |
|--------------------------------------|-----------|--------------------|------|-------|----------------|---------------------|------|-------|----------------|
| | | ME | RMSE | CV | R ² | ME | RMSE | CV | R ² |
| Sand content (% in weight) | SoilGrids | -0.906 | 18.6 | 0.457 | 0.518 | -0.27 | 19.1 | 0.501 | 0.492 |
| | GSDE | -0.443 | 23.2 | 0.571 | 0.247 | -1.31 | 23.8 | 0.625 | 0.211 |
| | HWSD | 6.64 | 27.4 | 0.673 | 0.014 | 2.08 | 27.6 | 0.725 | -0.058 |
| | IGBP | 3.74 | 26.3 | 0.647 | 0.051 | 4.06 | 26.3 | 0.691 | 0.055 |
| Clay content (% in weight) | SoilGrids | 1.34 | 12.5 | 0.554 | 0.339 | 0.39 | 13.6 | 0.485 | 0.382 |
| | GSDE | -0.949 | 14.6 | 0.643 | 0.104 | -0.79 | 16.4 | 0.584 | 0.105 |
| | HWSD | 0.77 | 16.2 | 0.718 | -0.119 | 1.42 | 18.9 | 0.672 | -0.182 |
| | IGBP | 3.27 | 15.4 | 0.678 | 0.044 | 2.44 | 16.8 | 0.597 | 0.084 |
| Bulk density (kg/m ³) | SoilGrids | -79.7 | 237 | 0.164 | 0.338 | -33.5 | 212 | 0.136 | 0.327 |
| | GSDE | -68.4 | 279 | 0.193 | 0.030 | -65.5 | 269 | 0.173 | -0.043 |
| | HWSD | -105 | 298 | 0.206 | -0.033 | -168 | 317 | 0.204 | -0.107 |
| | IGBP | -55.6 | 273 | 0.189 | 0.050 | -112 | 294 | 0.189 | -0.130 |
| Coarse fragment (% in volume) | SoilGrids | 1.53 | 10.1 | 1.68 | 0.319 | 1.23 | 12.8 | 1.47 | 0.335 |
| | GSDE | 3.2 | 13.5 | 2.24 | -0.165 | 3.18 | 16.8 | 1.93 | -0.115 |
| | HWSD | 1.8 | 13.2 | 2.2 | -0.164 | -0.40 | 16.2 | 1.87 | -0.081 |
| Organic carbon (g/kg) | SoilGrids | 6.21 | 29.8 | 1.69 | 0.218 | 0.99 | 23.5 | 3.32 | 0.134 |
| | GSDE | -0.354 | 34.5 | 1.95 | -0.095 | 0.45 | 27.4 | 3.87 | -0.174 |
| | HWSD | -3.67 | 36.2 | 2.05 | -0.194 | -1.38 | 27.4 | 3.87 | -0.172 |
| | IGBP | 0.61 | 33.4 | 1.89 | -0.026 | 1.67 | 28.5 | 4.02 | -0.268 |

1355 *Quite a number of WoSIS soil profiles were considered in the compilation of the four products.
 1356 ME is the mean error. RMSE is the root mean squared error. CV is the coefficient of variation. R²
 1357 is the coefficient of determination.



1358
 1359 Figure 1 Soil sand and clay fraction at the surface 0-30 cm layer from SoilGrids, IGBP-
 1360 DIS and GSDE. The difference among them will lead to different modelling results for
 1361 ESMs. IGBP-DIS is Data and Information System of International Geosphere-Biosphere
 1362 Program, and GSDE is Global Soil Dataset for Earth System Model.



1363
 1364
 1365

Figure 2 Soil organic carbon and bulk density at the surface 0-30 cm layer from SoilGrids, GSDE and IGBP.